

### **Referee 1 general comment: 1- Timescale**

The development of the timescale is the crux of this study and it is clear that considerable effort has gone into the timescale. The paper makes it clear, without explicitly stating so, that the timescales was quite difficult to develop. I have great sympathy for anyone who develops ice-core timescales. However, the timescale as presented is not convincing for two reasons. First, the isotope sampling is too low to resolve annual layers for much of the core. At a sampling interval of 10cm (above 80m), this yields only 5 or 6 samples per year for much of the timescale given the accumulation rates. You need about twice that to resolve clear annual layers, especially on a proxy such as oxygen isotopes that have relatively noisy seasonal cycles. Statements like “no ambiguity in layer counting is detectable above 62.38 m (i.e. 1933 AD)” are in direct contradiction with the need to perform major ion analysis “for sections of unclear isotopic seasonality” and I can see ambiguity in Figure 2 (near 20 and 29 m depths).

It seems odd to me that for a relatively short core, the whole thing wasn’t sampled at much finer resolution (water isotope analyses are cheap and don’t need much ice) and that aerosol analysis wasn’t performed on the full core.

Second, the volcanic matches are not convincing. In Figure 4 it appears that any small peak that rises past the 2sigma level is considered a volcano if it happens to be of the correct age. This may be because the data are normalized before identifying volcanic peaks. Regardless of the normalization issue, using ECM (or sulfur) at coastal sites to identify volcanic events is very difficult because the volcanic signal gets overwhelmed by marine inputs.

The timescale is the crux of this paper. This means considerably more effort needs to be made to describe it convincingly, for both the annual layers and volcanic matches.

Items that this paper needs:

- 1) A clear description of what measurements were made at what depths (i.e. where were aerosols measured and show the ambiguities and how they were interpreted)
- 2) An analysis of the impact of the low sampling resolution on the ability to resolve annual layers (often, low resolution leads to picking false peaks)
- 3) A realistic assessment of annual-layer interpretation uncertainty
- 4) A critical assessment of volcanic matches. I.e. why is Cerro Azul 1932 not one of the bigger, yet unmatched, peaks about a meter above or below. (this same question applies to pretty much every match, except for possibly Tambora).
- 5) A description of why ECM loses the annual signal yet preserves the volcanic signal
- 6) Why Krakatau isn’t observable in the ECM record and what the distinctive characteristics in the aerosol record are that allow it to be identified. Also a description of why the technique to identify Krakatau wasn’t applied for the full core.

It sounds like the only truly identifiable volcanic event was Tambora. The authors need to make use of Tambora, and pattern with the unknown 1809 eruption, to make a strong case that this is indeed properly matched (Figure 4 does not do this). Plot it against high resolution ECM/Sulfur/Sulfate records of this event. If the authors can demonstrate that this is a clearly identifiable match, then it would strongly support their annual layer interpretation.

### **Author’s response:**

*We respond to this comment in three steps. First, we assess the referee’s comments concerning annual layer counting. Second, we discuss the volcanic matches. Third, we address each specific item that Referee 1 suggested we consider or implement.*

*First, we point out that the isotope sampling resolution reported in the original manuscript was not 10 cm everywhere above 80 m. To explore this, we have now calculated the number of samples per year and report these in Figure R1. Other studies have worked within this range (e.g., Schlosser and Oerter, 2002). We agree that it should be stated more clearly which resolution was used at which depth, and have now added the full isotope profile with a visual indicator*

of the resolution as two supplementary figures: Fig. S1 and Fig. S2. Ambiguities are now highlighted and discussed. At some depths, (e.g., between ~74 and 77 m) we increased the resolution to 5 cm, but – with an annual layer thickness of several tens of cm, in no case did the higher resolution data actually improve in the identification of annual layers. Therefore, we have not made more isotopic measurements. However, we did measure ECM at high resolution all along the core and this can be used to identify annual layers as well. It is a combination of both methods, supplemented by ionic measurements where available, that gives us confidence in our annual layer counting. For example, the ambiguities observed by Referee 1 “near 20 and 29 m depth” in  $\delta^{18}\text{O}$  are resolved at 20 m by looking at the synchronous peaks in  $\text{MSA}$ ,  $\text{nssSO}_4$  and  $\text{NO}_3^-$ , and at 29 m by looking at the synchronous peaks  $\text{NO}_3^-$ , ECM and the trough in the  $\text{Na}^+/\text{SO}_4^{2-}$  ratio. However, we do agree with the reviewer that ambiguities remain elsewhere, and this is precisely why we adopted (and have retained) the approach of two age estimates: youngest and oldest. The sentence “no ambiguity in layer counting is detectable above 62.38 m (i.e. 1933 AD)” has been removed. It is now stated that this method has a  $\pm 16$  year uncertainty at the base of the ice core. This new ‘uncertainty’ is the result of us considering the potential issues raised by Reviewer 1 and working through the entire record again in a more “conservative” way (described in Methods). Therefore, and despite the fact that the Tambora eruption still confirms the oldest estimate (see below), we added an analysis of the impact of this 16 years dating error on the trends reported in the paper in all figures and tables.

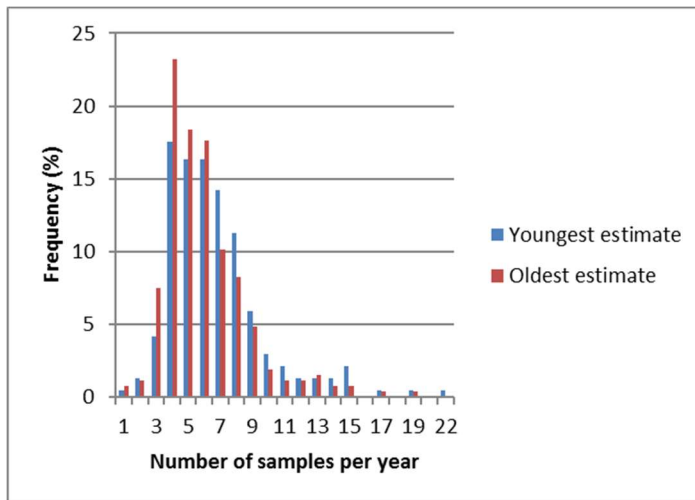


Figure R1. Distribution of the number of samples per year for the youngest and oldest estimates

Second, we agree with the referee that volcanic matching in a coastal ice core is, although not impossible (e.g. Kaczmarek et al., 2004), very difficult, even though we used ECM in combination with the annual layer counting. Therefore, we have chosen a simpler “conservative approach” along the lines suggested by the referee, i.e. only focusing on the Tambora eruption signature. In the revised manuscript we moved the high resolution ECM profile to a supplementary figure and added into the manuscript proper a figure centered on the depth range corresponding to where Tambora eruption should be visible, according to our two estimates (Fig.5). We also went back to the laboratory and made additional major ion measurements to document the Tambora eruption and show these on the same graph. We were very pleased to discover and report that there is only one peak that crosses the ECM 4 sigma threshold in the expected depth range and that it occurs at a depth corresponding precisely to our oldest age-depth estimate.

While these changes do not influence our conclusions, they do improve confidence in them and we thank Reviewer 1 for pointing us in this direction.

We now discuss each specific item suggested or requested by Referee 1:

1) A clear description of what measurements were made at which depths (i.e. where were aerosols measured and show the ambiguities and how they were interpreted)

*This is achieved by the full isotope profile as Fig. S1 and Fig. S2, including a visual indicator of the resolution and an explicit indication of the annual layer boundaries identified according to the two estimates.*

2) An analysis of the impact of the low sampling resolution on the ability to resolve annual layers (often, low resolution leads to picking false peaks)

5 *This is now done with the youngest estimate, which only interprets the minimum number of annual layers.*

3) A realistic assessment of annual-layer interpretation uncertainty

*This is also addressed by the youngest and oldest estimates.*

4) A critical assessment of volcanic matches. I.e. why is Cerro Azul 1932 not one of the bigger, yet unmatched, peaks about a meter above or below. (this same question applies to pretty much every match, except for possibly Tambora).

10 *As explained above, in the revised manuscript we have focused solely on identifying the most distinctive peak, that of Tambora. However, for information, the oldest estimate in our revised manuscript would now be 3 years older at the same depth and Cerro Azul does indeed correspond to the peak at 61 m. We do not discuss this in the revised manuscript since it occurs in a section of the core where the mismatch between our older and younger estimates is still reasonably low ( $\pm 2$  years).*

15 5) A description of why ECM loses the annual signal yet preserves the volcanic signal

*ECM loses the annual signal and the volcanic signal only in some sections of the record, e.g. between 83 and 85 m. This could result from a variety of factors that we do not discuss because ECM seasonality is only used as a back-up where needed and not as a primary source of information.*

20 6) Why Krakatau isn't observable in the ECM record and what the distinctive characteristics in the aerosol record are that allow it to be identified. Also a description of why the technique to identify Krakatau wasn't applied for the full core.

It sounds like the only truly identifiable volcanic event was Tambora. The authors need to make use of Tambora, and pattern with the unknown 1809 eruption, to make a strong case that this is indeed properly matched (Figure 4 does not do this). Plot it against high resolution ECM/Sulfur/Sulfate records of this event. If the authors can demonstrate that this is a clearly identifiable match, then it would strongly support their annual layer interpretation.

25 *The characteristics of a volcanic peak are now shown only for Tambora, with  $\text{nssSO}_4$  and  $\text{SO}_4^{2-}/\text{Na}^+$ , that also show a peak, outside the seasonal variations and synchronous with the ECM record. We agree with the referee in believing that the ECM signal is potentially subject to too much influence by marine inputs to act as an unambiguous indicator for many of the other peaks. We thank the reviewer for these observations and the Methods and Discussion sections of the revised manuscript have been changed accordingly.*

30 *The Tambora peak and the associated ion record can now be seen in Fig. 5. No other peak above or below could be associated with this eruption. We associate it to a clear peak in  $\text{SO}_4^{2-}/\text{Na}^+$  which occurs between two seasonal peaks and corresponds to high  $\text{nssSO}_4$  value (3.3 times higher than the mean). We believe this new conservative approach is scientifically robust and lends strength to our oldest estimate of the time scale involved.*

35 **Referee 1 general comment: 2- Description of the layer thinning correction**

The corrections for flow-induced layer thinning reveal a lack of understanding of how ice flow and are clearly underestimated. In particular, it is disappointing that the authors don't make use of the detailed ice-flow modeling that's been done on Derwael Ice Rise (Drews et al., 2015) to develop the vertical thinning function. It is clear from phase sensitive radar measurements (Kingslake et al., 2014) that the simple approximations for vertical thinning have trouble replicating the vertical strain pattern under ice divides.

40 The Nye assumption is so obviously not applicable to Derwael Ice Rise, which has a distinctive Raymond Bump, that it should not even be considered. The authors don't supply the kink height value of the D-J model. Using a kink height

of nearly 1, Kingslake et al. could still not match the pattern under Roosevelt Island. Since the authors say the kink height is below the zone of interest, I can infer that they didn't use anything greater than  $\sim 0.7$ . This will lead to an underestimation of the amount of strain experienced by the ice in the core. Thus the older accumulation rates will be underestimated, and it will appear that there has been an increase in modern accumulation rates. The underestimation is likely exacerbated by the preferred thinning rate of 3cm per year for the ice rise (Drews et al., 2015). Getting the thinning right is critical to primary conclusion of this paper.

### **Author's response**

*We thank the referee for this remark, which is certainly relevant and important. However, as we will show below, the effect of taking the Raymond effect into account does not alter the main conclusions of the manuscript.*

*First, we removed the Nye time scale approach from the revised manuscript, which is – as rightly pointed out by the referee – much too simplistic to be valid at the ice divide of an ice rise (we actually initially chose to show it to demonstrate the importance of using a more refined and adequate approach). Also as suggested by the reviewer, we took the vertical velocity profile from Drews et al. (JGR, 2015), which takes into account the Raymond effect on the Derwael Ice Rise through a full Stokes approach, as well as a slight amount of thinning (although the thinning is not the main factor to obtain the best fit) and ice anisotropy. This Drews profile indeed yields the best match with radar layers at depth. However, the Drews et al. (2015) strain rate profile used a mean accumulation rate that is somewhat lower than the long-term accumulation rate we obtain from the ice core. In order to determine the long-term accumulation rate we relied on an independent measure of horizontal surface strain measured on the Derwael Ice Rise. From a hexagonal strain network, we calculated horizontal strain rates ( $\epsilon_{xx} + \epsilon_{yy}$ ) to be equal to  $0.002 \text{ a}^{-1}$ . Mass conservation then gives a vertical strain rate at the surface of  $-0.002 \text{ a}^{-1}$ . The vertical velocity profile was then scaled to match the measured vertical strain rate at the surface. A best fit to the measured radar layers was obtained with a value of a mean accumulation rate of  $0.55 \text{ m a}^{-1}$  ice equivalent (see Fig. R2 below and Fig. 2 in the revised manuscript).*

*As an alternative approach, we used the Dansgaard-Johnsen model to fit the characteristics at the ice divide, as exhibited by the Raymond effect. Assuming that the horizontal velocity is zero, the vertical velocity is maximum at the surface, where it equals the accumulation rate (with negative sign), and is zero at the bed. Assuming a vertical surface strain rate of  $-0.002 \text{ a}^{-1}$ , we can determine the location of the kink point (between constant strain rate above and a strain rate linearly decreasing with depth below) that obeys these conditions (Cuffey and Paterson, 2010). This approach indicates that the kink point lies at  $0.9H$ , where  $H$  is the ice thickness. As seen in Fig. 2b, this method yields a vertical strain pattern that is consistent with that of Drews et al. (2015), especially in the first 120 m corresponding to the length of the ice core.*

*Both strain rates (Drews/D-J) were then used to correct the ice equivalent layer thickness for strain thinning. Layer thicknesses were then converted in from ice equivalent to w.e. for easier comparison with other studies.*

*While these results still conform to the previous conclusions of the paper, they are more robust and we thank the reviewer again for raising this issue. Figure 6 of the revised manuscript has been adapted to include this new, more physically sound, approach. We would like to point out that this paper is one of the few that actually investigates the impact of deformation on annual layer thicknesses in such details. We also now include Reinhard Drews as one of the co-authors.*

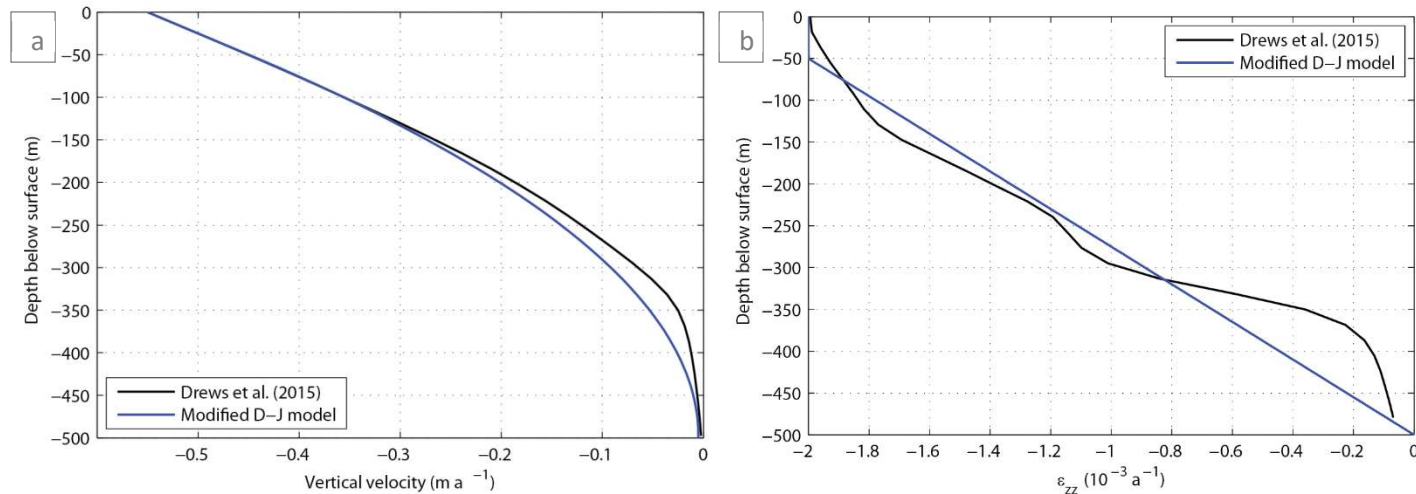


Figure R2. Vertical velocity (a) and vertical strain rate (b) profiles, according to the modified Dansgaard-Johnsen model (blue) and the full Stokes model (black, Drews et al., 2015).

### Referee 1 general comment: 3- Climate implications

- 5 The discussion of atmospheric and sea-ice patterns seems like an after thought. I'm not sure why the authors choose to analyze only anomalously high and low years. I also wonder why the authors don't compare the inferred accumulation rate history to the climate reanalyses. Other cores (e.g. Medley et al., 2013, GRL; Morris et al., 2015, Nature Geosciences) find good correlation of annual accumulation.

### Author's response:

- 10 In the revised manuscript, we have framed the discussion of the relation between core-derived SMB and climate parameters better. We now compare the ice-core-derived SMB with P-E estimates from ERA-Interim and RACMO2. The correlation is moderate for both ( $R^2=0.36$  and  $0.5$  for ERA-Interim and RACMO2, respectively), compared to other ice cores in West Antarctica, which indicates that local wind-induced snow redistribution and sublimation are significant contributors to local SMB at the ice core site (Lenaerts et al., 2014). Subtle variations in wind speed and direction could lead to strong perturbations of the snow accumulation, especially at a wind-exposed site such as Derwael Ice Rise. However, it is unlikely that the wind has an impact on the temporal trend observed in IC12. Unfortunately, our methods do not allow explicit partitioning of the SMB explained by precipitation vs. wind processes. Therefore, we compared with CESM rather than with the reanalyses data because (1) it yields an SMB and climate time series that overlaps substantially with the ice core record (1850-2012), unlike the reanalyses that only covers ~35 years, and (2) the present-day climate and SMB are realistic (Lenaerts et al., 2016). This is now clearly indicated in the text of the revised manuscript.
- 20

We now address the specific comments made by Referee 1.

Referee 1 specific comments	Author's response
P1, L27-29 – your data do not actually support this because your thinning correction is much too small.	We revised the complete strain correction by using the Drews et al. (2015) strain rates and a modified D-J model (discussed in detail above). Both are further constrained by measured surface horizontal strain rates. This amendment has not altered our conclusions.
P2, L10 – you should mention timescales. Frieler et al only address glacial-interglacial changes. The most directly comparable ice-core record to yours is from Law Dome, which does not show a consistent	We added the precision “during glacial-interglacial changes” and took more care at mentioning timescales in the revised manuscript.

relationship between accumulation and temperature in the Holocene.	
P3,L1 – in the ice-core community, continuous is generally used to mean a melting system where discrete samples are not cut. Using continuous to mean that all of the core has been sampled discreetly is confusing.	<i>Amended</i>
P3,L13 – Be specific about what you mean by local ice flow. You should really mention that it's an ice rise with a well developed Raymond Bump that has likely been stable for thousands of years.	<i>This is now described in Paragraph 2.1</i>
P4,L25 – DC-ECM does not depend on the impurity content at the crystal boundaries. It depends on the acidity.	<i>Rectified</i>
P4,L28 – a ~30cm smoothing window seems really large to me.	<i>We also tested with a smaller smoothing window (101 and 201) and we chose 301 points in an attempt to reduce the noise from the marine input. This does not have an impact on the Tambora volcanic horizon we discuss.</i>
P5,L1-3 – Did you normalize the data before identifying the volcanic peaks? If so, you can no longer reliably identify volcanic events with a threshold because the increased conductance of volcanic events would impact the normalization. Is the 2sigma threshold then for the entire data set. I'm confused, but I think this is a major problem.	<i>We applied the method described in Karlof et al. (2000) and Kaczmarska et al. (2004): "The Savitsky-Golay filter eliminates peaks created due to random noise or short-term chemistry events but preserves peaks expected from volcanic events." We now use a <math>4\sigma</math> threshold instead of the <math>2\sigma</math>.</i>
P5,L5-22 – This section should be entirely redone. Get a thinning function from the ice-flow modelers working on Derwael Ice Rise.	<i>Amended (discussed in detail above)</i>
P6,L17 – explain what changes in the ECM and why	<i>We changed the sentence by: "For ECM, there is also a regular seasonal signal, but it becomes very noisy below 80 m, although some seasonal cycles can still be seen for example between 115 and 118 m (Suppl. Fig. 1)"</i>
P6,L27 – explain how Krakatau was identified	<i>This sentence was removed. See response to general comment nr 1, specific items nr 6.</i>
P10,L11 – why are the uncertainties being presented after the results	<i>We modified the structure of the discussion and moved the paragraph about uncertainties to the end of the Results section.</i>
P10,L30 – there is a lot complexity in the position of the divide, the Raymond Bump, and the minimum accumulation (which is offset from the divide). There needs to be a much more detailed discussion of whether small (i.e. one ice thickness)	<i>This comment has been clipped (the last sentence is not finished) but we understand that the reviewer suggests we explain the small-scale variability of the SMB near ice divides in more detail. We have amended sections 2.1 and 3.3 accordingly.</i>

## Referee 2 general comments:

I have only basic knowledge in dating ice cores using flow models, so I cannot assess the critics of referee #1 considering this point. The authors do show both the uncorrected data and the correction with the different models, so the reader can assess what they have done. Also, their main conclusion (positive SMB trend in the last 100 years) would still be valid for any calculation of layer thinning that lies between the two methods they use.

However, I share Referee #1's doubts about the details of the dating, particularly the use of volcanic horizons, since the attribution of the ECM peaks in Figure 4 to the different eruptions is not convincing, except for Tambora. Also, the authors do not give details about the layer counting using stable isotopes, to which depth this was possible etc. Nobody expects a perfect dating of an ice core because this hardly ever exists.

However, I think the authors should discuss the error possibilities of the dating a bit more and give a more realistic quantitative estimate of the error. Probably, within the error bounds, their main result would hold. But, see above, I cannot assess the details of the used models. The authors state that their findings (increase in SMB in a coastal East Antarctic core) are the first ones that support model predictions. This does not make them discuss how representative their results are. They compare their results with other firn/ice cores, but do not compare the temporal variations of the SMB derived from the core with temporal variations of measured and/or modelled air temperature, sea ice, or surface pressure data). Instead they look at composites for very positive and very negative years, which is, in principal, not a bad thing to do, but I would expect stronger signals here in order to be convincing. The arguments using the output from the Community Earth System Model are a bit weak. The discussion of the atmospheric dynamics involved is not clear and mixes up conditions at the coast and in the interior of Antarctica. Also, different time scales are mixed together and often it is not clear, which time period is meant when certain trends are reported.

## Author's response to referee 2's general comments:

*We decided to follow the advice of the referees and removed the detailed volcanic matching, except for Tambora (described in detail above). We also include an assessment of the impact of the 16 years dating uncertainty in all graphs and tables and in the main text to show that it does not change our conclusions.*

*As outlined in our response to Referee 1, there is a moderate temporal correlation between the SMB from the ice core and the SMB from climate reanalyses, which suggests that wind processes influence local SMB at Derwael Ice Rise. The relationships between precipitation and sea ice, SST and large-scale circulation are analyzed using output from the Community Earth System Model (CESM). CESM was selected for two reasons: (1) it yields an SMB and climate time series that overlaps to a great extent with the ice core record (1850-2012), unlike the reanalyses that only cover ~35 years, and (2) the present-day climate and SMB are realistic (Lenaerts et al., 2016). This is now more clearly indicated in the text.*

*We thank the reviewer for the suggestion on the significance of the signals that are found in low and high accumulation years. We have now compared the anomalies in those years with the temporal standard deviation, and adapted ex-Figure 7 (now Fig. 8) such that signals are only shown where they are larger than one standard deviation. Clearly, the signals exceed the standard deviation for the high anomaly years, but are not significant for the low accumulation years. Therefore, we decided to omit the bottom panel and only show the situation in the high accumulation years.*

Referee 2 Specific comments	Author's response
Title: what does "recent" mean? and, to be correct, "snow accumulation" should be "surface mass balance".	<i>The title has been changed to: "Ice core evidence for a 20<sup>th</sup> century increase in surface mass balance in coastal Dronning Maud Land, East Antarctica."</i>
Abstract: It would be good to re-write the abstract after the main text has been revised.	<i>Agreed and done.</i>

P2:	
L5: increasing ice discharge	<i>Amended</i>
L8: What does the Polvani paper have to do with warming- related increase in precip? There are other papers that involve data and modelling and do not find either warming or increase in precipitation in the considered period. Please, make sure that it is clear about which time period you are talking.	<i>We deleted the Polvani reference and added a sentence acknowledging papers that do not find warming, except in West Antarctica. Papers that do not find an increase in SMB were already mentioned. We added precisions of the periods considered.</i>
L23: “both authors concluded that the trends were insignificant”. This is not correct and not exact. Which trends? Altnau et al. found a statistically significant positive trend in SMB for the interior DML.	<i>We apologise for the confusion. The sentence has been changed to “Frezzotti et al. (2013) showed no significant SMB changes over most of Antarctica since the 1960s, except for an increase in coastal regions with high SMB and the highest part of the East Antarctic ice divide, and Altnau et al. (2015) found a statistically significant positive trend in SMB for the interior DML.”</i>
P3:	
L10ff: grammar: in your sentence, “which” refers to the project.	<i>The sentence has been changed accordingly.</i>
L12: a local flow regime	<i>Amended</i>
How high is the accumulation rate? It would be good to give this information already here.	<i>We added this information and chose to use the previously published accumulation rate of 0.50 m w.e. (0.55 m i.e., Drews et al., 2015).</i>
P4:	
L3: do you mean 30mm x 30mm?	<i>Yes, amended.</i>
L13: the boundary between annual layers	<i>Amended</i>
L21: better: were carried out	<i>Amended</i>
P5:	
L5: snow burial: better: the compression of the snow under its own weight	<i>Amended</i>
It would be interesting to see the density profile here, maybe you could add this in a figure. I also miss some information about the depth until which seasonal variations in the isotope ratios can be resolved.	<i>We think that adding the density profile in a figure is not necessary, since it is published in Hubbard et al., 2013. However, if the referee or Editor believes this would improve the quality of the paper, we are ready to do it.</i>
P6:	
L3: how reliable are the CESM data for the 19th century, especially sea ice?	<i>That is a very good question. In fact, we have little to no observational estimates of 19<sup>th</sup> century sea-ice extent. The CESM simulated sea-ice extent in the observational period is very realistic compared to observations (Lenaerts et al., 2016) and does not show any trend in the Atlantic sector, which gives us confidence that the sea ice is treated realistically.</i>
L24: better: mainly derived from. . .	<i>Amended</i>
P7:	
L1ff: see above. The volcanic peaks in Figure 4 seem to be pretty ambiguous in most cases.	<i>The correspondence with volcanic peaks has been completely revised (addressed in detail above)</i>
P8:	
L15ff: This is a very short and simplified view. The sea ice argument is not convincing, especially the hatched area of anomalies is fairly small and should not have a large impact on precipitation amounts. A decrease in surface pressure of not much more than 1hPa is not very much, even in a composite, and in that case, lower surface pressure does not necessarily mean higher precipitation. I'll get back to that in the discussion part.	<i>We do not agree entirely with the statement that the anomalies are fairly small. We find a maximum anomaly of sea ice extent of more than 30 days, which is much larger than the inter-annual variability. We agree that the surface pressure anomaly is fairly small; we have revised the text according the reviewers' comments (see below).</i>



L26: define “current”, please.	<i>“current” was replaced by “recent”.</i>
P9:	
L2: How do you define “climate-related”? What else could it be on this time scale? Could it be that the first in-situ validation of increased precipitation in coastal Antarctica is due to the fact that the drilling location is influenced rather locally? Did you compare it with temperature proxies? I am not saying it is wrong or right what you state, but you should discuss this.	<i>We removed the term “climate-related”. We now discuss the spatial significance of our results at greater length.</i>
L8: strange usage of “refer to”. Maybe better “represents” or similar.	<i>Amended</i>
L13ff. Decreasing trend: I assume you mean “negative trend”. Decreasing would mean getting stronger negative with time.	<i>Amended</i>
Please, make sure that it is clear, which time period is considered in your respective comparisons.	<i>We agree that it was not clear and replaced all references to “the recent period” by “the last 50 years” and the “most recent period” by “the last ~20 years”.</i>
L10: Stenni et al: 1992-1996: too short a period to consider any trend calculation	<i>Reference to this has been deleted</i>
P10:	
L5. What is the reason for the choice of the threshold? Many coastal stations have SMBs around 0.3. This seems a bit arbitrary.	<i>This threshold was chosen in order to be consistent with Frezzotti et al. (2013) (no threshold allows isolation of only coastal stations)..</i>
L9: this is covered by only two high accumulation sites..	<i>Amended</i>
L14: dating accuracy	<i>Amended</i>
P11:	
L4ff: the positive trend in SMB. . . the result of various forcings	<i>Amended</i>
L7: the air does not “hold vapor”, a higher temperature means a higher saturation vapor pressure.	<i>Amended</i>
L7ff: Paragraph 4.3 is very important, but, unfortunately, it contains quite a few misconceptions (in spite of the fact that one of the co-authors is a meteorologist and expert for polar/Antarctic meteorology) and thus should be re-written: First of all, there is quite a bit of confusion of coastal and continental conditions. Several papers are quoted, of which some deal with the interior and others with the coastal areas of Antarctica, which, however, have very different precipitation regimes. Amplified Rossby waves are particularly important for precipitation in the interior of the continent, NOT for the coast. The coastal areas are always under the influence of synoptic activity in the circumpolar trough. The individual events quoted in line 18 can bring up to 50% of the total accumulation in the interior, not at the coast. And also this means the sum of all events, not one single event. 2009 and 2011 were years with such events in the interior, which of course, also bring high precipitation to some coastal areas, but are not necessarily associated with lower surface pressure, on the contrary, the pressure in the coastal areas of Antarctica is usually lower in years like 2010, where a zonal flow was predominant and the interior of the continent got less precipitation than on average.	<i>We agree with the reviewer that this part should be more concisely written, and that we should discriminate better between coastal and interior regions. We have revised the text accordingly.</i>

L25ff: SAM: what was the temporal resolution of your comparison of SAM, SOI and your data? Annual means, monthly values? You should not expect any signal in the annual mean since the SAM index has high intra-annual variations.	<i>This was indeed a comparison of annual mean, but we decided to delete this sentence, since it is not relevant.</i>
P12:	
L 4ff: you discuss topographic influences here, but never question that the result for the ice rise might be more locally influenced than climate-related (whatever that means). The topography of an ice rise influences the synoptically caused winds much more than the surrounding ice shelf or the plateau since the ice rise represents a disturbance in the main flow. This is especially surprising since the authors include the Lenaerts et al. J. Glac.2014 paper, which investigates the climate and mass balance on ice rises, in the reference list, but never discuss it in the text.	<i>We appreciate the reviewers comment, and we agree with it. In the revised manuscript we now include discussion of the local wind effects on the SMB.</i>
L19: what do you mean by “these two highly variable accumulation events”?	<i>Sentence amended</i>
L20: what is the physical explanation for DML being most susceptible to an increase in snowfall in a warmer climate? So far, a positive trend in Antarctic sea ice has been observed, which according to your findings, should decrease precipitation. (not sure about the regional trends, though, I am no sea ice expert.)	<i>Lenaerts et al. (2016) attributed future increase in DML snowfall partly to increasing temperature and partly to a simulated future decrease in sea ice extent. The observational record does not show any significant changes in sea-ice in the Southern Ocean region around 30-70 °E (e.g. Bintanja et al., 2013). However, although global sea ice area does appear to be increasing slightly in the Southern Ocean, several studies show that it this general expansion hides strong regional differences. Indeed, Stammerjohn et al. (2009) showed that the Princess Ragnhild coast area and, more generally, the Southern Ocean to the East of it, show a recent slight reduction of the sea ice season duration. This is part of a circum-antarctic bipolar pattern similar to the SAM spatial distribution.</i>
L24ff: see general comment. What is the temporal resolution of the investigation of the relationship between SAM, SOI and SMB?	<i>This comment is not linked to P.12, L24. Anyway, we removed the investigation of the correlation between SAM, SOI and our observed SMB data from the revised manuscript..</i>
L26ff: Low pressure: see above. Usually the pressure in the circumpolar trough is lower (on average) in years with more zonal flow and less meridional heat and moisture exchange (positive SAM index) than in years with amplified Rossby waves.	<i>That is correct, and we apologize for the misinterpretation. Since the anomalies in surface pressure are smaller than the standard deviation, we decided to omit these from the Figure and revised text.</i>
P13:	
L4: positive trend	<i>Amended</i>
L12ff: I do agree that the ice rise is a suitable potential drilling site for a longer core. However, you should investigate the representativeness of your results a bit closer and keep this in mind when interpreting a deeper core	<i>The discussion has been amended accordingly.</i>
References: The reference list contains quite a few publications that are not quoted in the text. Please, check.	<i>Thank you, we checked the reference list and removed the errors. There are still a few references that are not quoted in the text. This is because they are referred to in Table A1, and therefore, used in Figure 1.</i>

	<i>These are: Anschutz et al., 2009; Ekaykin et al., 2004; Frezzotti et al., 2007; Igarashi et al., 2011 ; Jiang et al., 2012; Morgan et al., 1991 ; Mulvaney et al., 2002 ; Roberts et al., 2015; Ruth et al., 2004 ; Schlosser et al., 2014; Sommer et al., 2000; Stenni et al., 1999; Takahashi et al., 2009; van Ommen and Morgan, 2010; Xiao et al., 2004; Zhang et al., 2006.</i>
P16: L15: new paragraph: Hofstede. . .	<i>Amended</i>
P20: l25; new paragraph: Schlosser. . .	<i>Amended</i>
P26: the caption of Figure 26 should be rephrased: “Diff. in mean annual SMB between ~1960-present and ~1816 –present (a,b)” (c,d accordingly)	<i>Amended</i>
P31: Figure 6: a) b) labels missing	<i>Amended</i>
The legend is a bit confusing, since the dotted lines claim to be a mean SMB, only the caption explains that it is mean plus/minus STD. Maybe a single line with some shading for the range of the STD would be show this more clearly. For 1992 to 2012, one would expect that the averages are not very different, given the closeness of the green and the black line?	<i>The Figure has now changed completely (discussed above). Since most volcanic horizons are not used as reference markers anymore, Figure 7 now illustrates the rate of change between fixed periods of 20 and 50 years.</i>

## References in response

- 5 *Bintanja, R., van Oldenborgh, G. J., Drijfhout, S. S., Wouters, B., & Katsman, C. A.: Important role for ocean warming and increased ice-shelf melt in Antarctic sea-ice expansion. Nature Geosci., 6(5), 376–379. doi:10.1038/ngeo1767, 2013.*
- 10 *Lenaerts, J. T. M., Brown, J., Van Den Broeke, M. R., Matsuoka, K., Drews, R., Callens, D., ... and Van Lipzig, N. P. M.: High variability of climate and surface mass balance induced by Antarctic ice rises. J. Glaciol., 60(224), 1101–1110. doi:10.3189/2014JoG14J040, 2014.*
- 15 *Stammerjohn, S.E., Martinson, D.G. Smith, R.C., Yuan, X., and Rind, D.: Trends in Antarctic annual sea ice retreat and advance and their relation to El Niño–southern oscillation and southern annular mode variability, J. Geophys. Res., 113, p. C03S90 <http://dx.doi.org/10.1029/2007JC004269>, 2008.*

# Ice core evidence for a recent-20<sup>th</sup> century increase in snow accumulation surface mass balance in coastal Dronning Maud Land, East Antarctica

Morgane Philippe<sup>1</sup>, Jean-Louis Tison<sup>1</sup>, Karen Fjøsne<sup>1</sup>, Bryn Hubbard<sup>2</sup>, Helle A. Kjær<sup>3</sup>, Jan T. M. Lenaerts<sup>4</sup>, Reinhard Drews<sup>5</sup>, Simon G. Sheldon<sup>3</sup>, Kevin De Bondt<sup>6</sup>, Philippe Claeys<sup>6</sup>, Frank Pattyn<sup>1</sup>

<sup>1</sup>Laboratoire de Glaciologie, Département des Géosciences, Environnement et Société, Université Libre de Bruxelles, BE-1050 Brussels, Belgium

<sup>2</sup>Centre for Glaciology, Department of Geography and Earth Sciences, Aberystwyth University SY23 3DB, United Kingdom

<sup>3</sup>Centre for ice and climate, Niels Bohr Institute, University of Copenhagen, Juliane Maries Vej 30, 2100, Copenhagen, Denmark

<sup>4</sup>Institute for Marine and Atmospheric research Utrecht, Utrecht University, Princetonplein 5, 3584 CC Utrecht, Netherlands

<sup>5</sup>Bavarian Academy for Sciences and Humanities, Alfons-Goppel-Strasse 11, 80539 Munich, Germany

<sup>6</sup>Department of Analytical Environmental and Geo-Chemistry, Vrije Universiteit Brussel, Pleinlaan 2, BE-1050 Brussels, Belgium

Correspondence to: M. Philippe (mophilip@ulb.ac.be)

**Abstract.** Ice cores provide temporal records of snow-accumulation Surface Mass Balance (SMB), a crucial component of Antarctic mass balance. Coastal areas are particularly under-represented in such records, despite their relatively high and sensitive accumulation rates. Here we present records from a 120 m ice core drilled on the Derwael Ice Rise, coastal Dronning Maud Land (DML), East Antarctica in 2012. Water stable isotopes ( $\delta^{18}\text{O}$  and  $\delta\text{D}$ ) stratigraphy is supplemented by discontinuous major ion profiles and continuous electrical conductivity measurements (ECM). The ice core and the identified Tambora 1815 volcanic horizons confirm the dating. We date the core bottom to 1759  $\pm$  16 A.D. 17435  $\pm$  2 AD and for the ice core bottom the identified Tambora 1815 volcanic horizons confirm the oldest age-depth estimate.  $\delta^{18}\text{O}$  and  $\delta\text{D}$  stratigraphy is supplemented by discontinuous major ion profiles, and verified independently by electrical conductivity measurements (ECM) to detect volcanic horizons. The resulting annual layer history is combined with the core density profile to calculate-reconstruct SMB-accumulation history, corrected for the influence of ice deformation. The mean long-term accumulation rate is 0.4725  $\pm$  0.0235 m water equivalent (w.e.) a<sup>-1</sup> (average-corrected-value). Reconstructed annual accumulation rates show an increase from 1955 onward in the last 50 years to a mean value of 0.61  $\pm$  0.012 m-w.e. a<sup>-1</sup> between 196255 and 20112. This trend is compared with other reported

Formatted: Left: 0.98", Right: 0.98", Top: 0.98", Bottom: 0.98", Footer distance from edge: 0.51"

Formatted: Superscript

Formatted: Superscript

Formatted: Superscript

Formatted: Not Superscript/ Subscript

Formatted: Not Superscript/ Subscript

Formatted: Not Highlight

Formatted: Not Highlight

Formatted: Not Highlight

Formatted: Not Highlight

Formatted: Not Highlight

Formatted: Not Highlight

Formatted: Not Highlight

Formatted: Not Highlight

accumulation data in Antarctica, generally showing a high spatial variability. ~~Output of the fully coupled Community Earth System Model demonstrates that sea ice and atmospheric patterns largely explain the accumulation variability. This is the first record from a coastal ice core in East Antarctica showing a steady increase during the 20<sup>th</sup> and 21<sup>st</sup> centuries, thereby supporting modelling predictions. Output of the fully coupled~~  
5 ~~Community Earth System Model suggests that variability in sea surface temperatures and sea ice cover in the precipitation source region explain part of the variability in SMBSMB, along with a likely significant impact of local snow redistribution.~~ The latter ~~which likely has a significant impact on interannual variability but not on long-term trends. This is the first record from a coastal ice core in East Antarctica showing a steady increase of accumulation rates during the 20<sup>th</sup> and 21<sup>st</sup> centuries, thereby supporting modelling predictions.~~

Formatted: Superscript

Formatted: Superscript

## 1 Introduction

In a changing climate, it is important to know the Surface Mass Balance (SMB, i.e. precipitation minus evaporation, sublimation, meltwater runoff, and/or erosion) of Earth's ice sheets as it is an essential component of their total mass balance, directly affecting sea level (Rignot et al., 2011). The average rate of Antarctic contribution  
15 to sea level rise is estimated to have increased from 0.08 [−0.10 to 0.27] mm a<sup>−1</sup> for 1992–2001 to 0.40 [0.20 to 0.61] mm a<sup>−1</sup> for 2002–2011, mainly due to increasing rising ice discharge from coastal West Antarctica (Vaughan et al., 2013).

Formatted: Not Highlight

This increase in dynamic ice loss could be partly balanced by a warming-related increase in precipitation ~~in East Antarctica~~ (e.g. Polvani et al., 2011; Krinner et al., 2007; Palermé et al., 2016) by the end of the 21<sup>st</sup> century. There  
20 is consistent evidence that past Antarctic snow accumulation rates (used as a synonym for SMB) were positively correlated with past air temperature during glacial–interglacial changes, as recently shown by Frieler et al. (2015) using ice core data and modelling. The present-day warming seems to be confined to West Antarctica (Turner et al., 2005; Bromwich et al., 2014; Ludescher et al., 2015) and there is no significant long-term trend in the SMB  
25 over the continent during the past few decades (Van de Berg et al., 2006; Monaghan et al., 2006; van den Broeke et al., 2006; Bromwich et al., 2011; Lenaerts et al., 2012; Wang et al., 2016). However, ~~sThere is consistent evidence that past Antarctic snow accumulation rates were positively correlated with past air temperature, as recently shown by Frieler et al. (2015) using ice core data and modelling. Similarly, satellite radar and laser altimetry suggest recent mass gain in East Antarctica (Shepherd et al., 2012). Dronning Maud Land (DML) in particular, which has experienced several high-accumulation years since 2009 (Boening et al., 2012; Lenaerts et~~

Formatted: Not Highlight

Formatted: Superscript

Formatted: Not Highlight

Formatted: Not Highlight

Formatted: Not Highlight

al., 2013). ~~C, in particular in DML, which has experienced several high accumulation years since 2009 (Boening et al., 2012; Lenaerts et al., 2013). However, although recent alibrated regional atmospheric climate models indicate higher accumulation during 1980–2004 along the coastal sectors than in previous estimates (e.g. Van de Berg et al., 2006), they show~~, Wang et al. (2016) found that climate models generally underestimate SMB in coastal DML. ~~DML, which has experienced several high accumulation years since 2009 (Boening et al., 2012; Lenaerts et al., 2013); no long-term trend in the total accumulation over the continent during the past few decades (Monaghan et al., 2006; van den Broeke et al., 2006; Bromwich et al., 2011; Lenaerts et al., 2012).~~

Ice cores provide temporal records of snow accumulation, ~~which~~. ~~These~~ are essential to calibrate internal reflection horizons in radio-echo sounding records (e.g. Fujita et al., 2011; Kingslake et al., 2014), to force ice sheet flow and dating models (e.g. Parenin et al., 2007) and to evaluate regional climate models (e.g. Lenaerts et al., 2014). However, records of accumulation are still scarce relative to the size of Antarctica. While ~~est~~ the majority ~~laek~~ ~~ashow~~ ~~no~~ significant trend in snow accumulation over the last century (e.g. Nishio et al., 2002), some do show an increase (e.g. Karlof et al., 2005), and others show a decrease (e.g. Kaczmarska et al., 2004). Frezzotti et al. (2013) compiled surface accumulation records for the whole of Antarctica and Altnau et al. (2015) for ~~Dronning-Maud-Land (DML)~~ ~~more specifically~~. Frezzotti et al. (2013) showed ~~no significant SMB changes over most of Antarctica since the 1960s, except for an increase in coastal regions with high SMB and in the highest part of the East Antarctic ice divide~~. Altnau et al. (2015) found a statistically significant positive trend in SMB for the interior DML. ~~Both authors concluded that the trends are insignificant.~~

However, there is still a clear need for data from the coastal areas of East Antarctica (ISMASS Committee, 2004; van de Berg et al., 2006; Magand et al., 2007; Wang et al., 2016), where very few studies have focused on ice cores, and few of those have spanned more than ~~20–50~~ years. Coastal regions allow higher temporal resolution as accumulation rates generally decrease with both ~~altitude-elevation~~ and distance from the coast (Frezzotti et al., 2005). Ice rises are ideal locations for paleoclimate studies (Matsuoka et al., 2015) as they are undisturbed by up-stream topography, ~~since-and~~ lateral flow is almost negligible. Melt events are also likely to be much less frequent than on ice shelves (Hubbard et al., 2013).

In this paper we report on ~~water stable isotopes (continuous ice~~  $\delta^{18}\text{O}$  and  $\delta\text{D}$ ) measurements (5–10 cm resolution) along a 120 m ~~ice~~ core drilled on ~~the~~ Derwaal Ice Rise (DIR) (~~70°14'44.88" S, 26°20'5.64" E~~), in coastal DML. This record is complemented by major ions ~~and continuous electrical conductivity measurement (ECM)~~ profiles to improve the resolution of the seasonal cycles wherever necessary. ~~Dating is checked independently using The identification of the volcanic horizon corresponding to the 1815 eruption of Tambora volcanic horizons allowed us to constrain the dating within an uncertainty of 2 years~~ ~~detected from continuous electrical conductivity~~

Formatted: Not Highlight

Formatted: Not Highlight

Formatted: Font color: Auto, Not Highlight

Formatted: Font color: Auto, Not Highlight

Formatted: Font color: Auto, Not Highlight

Formatted: Font color: Auto, Not Highlight

Formatted: English (United Kingdom)

measurements (ECM) along the core (Hammer et al., 1994). After correcting for dynamic vertical thinning, we derive annual accumulation, and average accumulation and trends over the last  $254 \pm 1667$  years, i.e. across the Anthropocene transition. These are compared with other reported trends in Antarctica, including DML, over the last decades and 50 years.

Formatted: Not Highlight

Formatted: Not Highlight

Formatted: Not Highlight

## 2 Field site and methods

### 2.1 Field site

The study site is located in coastal DML, East Antarctica. A 120 m ice core, named IC12 after the project name IceCon, was drilled in 2012 on the divide of the DIR (70°14'44.88"S, 26°20'5.64"E, 450 m a.s.l., Fig. 1). This ice rise is 550 m thick and the recent SMB has been estimated on the basis of remote sensing to 0.50 m w.e. a<sup>-1</sup> (Drews et al., 2015; Callens et al., 2016).

Formatted: Normal

Ice rises provide scientifically valuable drill sites because they are located close to the ocean (and hence sample coastal precipitation regimes) and because remote-sensing data can easily identify drill sites on a local dome that are relatively undisturbed by horizontal flow can be identified easily from remote-sensing data. However, a number of regional factors complicate the interpretation of ice-core records on ice rises: ice rises form topographic barriers with the capacity to block atmospheric circulation on otherwise flat ice shelves. Orographic precipitation can thereby result in significantly higher SMB values on the upwind sides of such ice rises, with corresponding precipitation shadows on the downwind side (Lenaerts et al, 2014). For the DIR in particular, the SMB on the upwind side is up to 2.5 times higher than on the downwind side (Callens et al., 2016). On top of this larger scale asymmetry, Drews et al. (2015) identified a small scale SMB oscillation near the divide, tentatively attributed to erosion at the crest, and subsequent redeposition on its downwind side. The observed SMB maximum is therefore offset by ~4 km from the topographic divide where the ice core was drilled. This means that the absolute values of the ice-core derived accumulation rates derived here, sample a regime where the SMB varies on short spatial scales. Moreover, Drews et al. (2015) identified isochrone arches (a.k.a. Raymond Bumps) beneath the divide. This characteristic flow pattern causes ice at shallow to intermediate depths beneath the divide to be older than at comparable depths in the ice-rise flanks, necessitating a specific strain correction for the ice-core analysis, which we discuss below. Both Drews et al. (2015) and Callens et al. (2016) suggested that the DIR has maintained its local ice divide for the last thousands of years and possibly longer. By matching the radar stratigraphy to an ice-flow model, Drews et al. (2015) suggested that the DIR divide elevation is close to steady-state and has potentially undergone modest surface lowering in the past. Both studies used a temporally constant SMB. Here we focus on

the temporal variability and argue that, because the DIR has been stable in the past, we can draw conclusion with respect to the larger-scale atmospheric circulation patterns.

The study site is located in coastal DML, East Antarctica. A 120 m ice core was drilled in 2012 on the divide of Derwael Ice Rise, named IC12 after the project name IceCon (70°14'44.88"S, 26°20'5.64"E Figure 1), which is 486 m thick and has a local ice flow (Drews et al., 2015). Due to its coastal location, the accumulation rate is high and allows dating by seasonal peak counting. Only a few very thin melt layers are present. A continuous density profile was obtained by calibrating optical televiewer (OPTV; Hubbard et al. 2008) luminosity records in the borehole with discontinuous gravimetric measurements (Hubbard et al., 2013).

## 2.2 Ice coring and density analyses

The IC12 ice core was drilled with an Eclipse electromechanical ice corer in a dry borehole. The mean length of the core sections recovered after each run was 0.77 m and the standard deviation 0.40 m. Immediately after drilling, temperature (Testo 720 probe, inserted in a 4 mm diameter hole drilled to the centre of the core, precision  $\pm 0.1$  °C) and length were measured on each core section, which was then wrapped in a PVC bag and stored directly in a refrigerated container at -25 °C, and kept at this temperature until analysis at the home laboratory. The core sections were then split bisected lengthwise in two, in a cold room at -20 °C. One half of the core section was used for ECM measurements and then kept as archive, while and the other half was sectioned for continuous-discrete stable isotope sampling (5–10 cm resolution on the whole core) and discontinuous-major ion analysis (5 cm resolution on discrete sections). The ice core is named IC12 after the project name IceCon. Only a few very thin (1 mm) ice layers are present. A continuous density profile using a best fit through discrete gravimetric measurements has been previously published (Hubbard et al., 2013) and is used here to convert measured annual layer thicknesses to meters water equivalent (w.e.) (Sect. 2.3) in the borehole with discontinuous gravimetric measurements (Hubbard et al., 2013).

## 2.3 Annual layer counting and dating

### 2.3.1 Water stable isotopes and major ionsmajor ion

Half of each core section was resampled as a central bar of 30 mm x 30 mm square section with a clean band saw. The outer part of the half-core was melted and stored in 4 ml bottles for  $\delta^{18}\text{O}$  and  $\delta\text{D}$  measurements, completely filled to prevent contact with air. For major ionsmajor ion measurements, the inner bar was then placed in a Teflon



holder and further decontaminated by removing ~2 mm from each face under a class-100 laminar flow hood, using a methanol-cleaned microtome blade. Each 5 cm-long decontaminated section was then covered with a clean PE storage bottle, and the sample cut loose from the bar by ~~hitting~~ striking it perpendicularly to the bar axis. Blank ice samples prepared from milliQ water were processed before every new core section and analysed for contamination.

5 Dating was achieved by annual layer counting identified from the stratigraphy of the  $\delta^{18}\text{O}$  and  $\delta\text{D}$  isotopic composition of  $\text{H}_2\text{O}$  measured (~~10 cm resolution in the top 80 m and 5 cm resolution below~~) with a PICARRO L 2130-i Cavity Ring Down Spectrometer (CRDS) (precision,  $\sigma = 0.05 \text{ ‰}$  for  $\delta^{18}\text{O}$  and  $0.3 \text{ ‰}$  for  $\delta\text{D}$ ). [This composition was measured at 10 cm resolution in the top 80 m and 5 cm resolution below \(See Fig. S1 for exact resolution\).](#) ~~The annual layer was identified by the  $\delta^{18}\text{O}$  summer maximum value.~~

10 For sections of unclear isotopic seasonality, major ion analysis ( $\text{Na}^+$ ,  ~~$\text{Cl}^-$~~ ,  $\text{SO}_4^{2-}$ ,  $\text{NO}_3^-$ , and methylsulonic acid (MSA))  ~~$\text{NO}_3^-$ ,  $\text{Cl}^-$~~  was ~~performed with~~ additionally carried out using a Dionex-ICS5000 liquid chromatograph. The system has a standard deviation of 2 ppb for  $\text{Na}^+$  and  $\text{SO}_4^{2-}$ , ~~8 ppb for  $\text{Cl}^-$~~ , 7 ppb for  $\text{NO}_3^-$ , and ~~1 ppb for MSA~~ ~~8 ppb for  $\text{Cl}^-$~~ . Non sea-salt sulfate was calculated as  $\text{nssSO}_4 = [\text{SO}_4^{2-}]_{\text{tot}} - 0.052 * [\text{Cl}^-]$ , following Mulvaney et al. (1992) and represents all  $\text{SO}_4^{2-}$  not of a marine aerosol origin. The ratio  ~~$\text{R}_{\text{Na}^+/\text{SO}_4^{2-}}$~~  was also calculated as an

15 indicator of seasonal  $\text{SO}_4^{2-}$  production.

Formatted: Not Superscript/ Subscript

Formatted: Not Superscript/ Subscript

Formatted: Not Superscript/ Subscript

### 2.3.2 ECM and volcanic horizons measurements

ECM measurements were ~~made~~ carried out in a cold room at  $-18^\circ\text{C}$  at the Centre for Ice and Climate, Niels Bohr Institute, University of Copenhagen, with a modified version of the Copenhagen ECM described by Hammer (1980). Direct current (1250 V) was applied at the surface of the freshly-cut ice and electrical conductivity was

20 measured at a 1 mm resolution. The DC electrical conductivity of the ice, once corrected for temperature, depends principally on ~~its impurity content located at the crystal boundaries~~ its acidity ( $\text{SO}_4^{2-}$ ,  $\text{NO}_3^-$ ,  $\text{Cl}^-$ , etc.) (Hammer, 1980; Hammer et al., 1994). This content varies seasonally and shows longer term localized maxima associated with sulfate production from volcanic eruptions. ECM can therefore be used both as a relative and an absolute dating tool.

25 [As measurements were principally made in firn, we applied a novel technique described by Kjær et al. \(in review\) to correct for the effect of the firn porosity on the noise amplitude of the signal. As the noise ECM current is low enhanced for higher air content, we multiplied the high resolution ECM signal by the inverse of the ice volume fraction, i.e. the ratio of the ice density to firn density \( \$\rho\_{\text{ice}}/\rho\_{\text{firn}}\$ \), us following the density profile from Hubbard et al. \(2013\).](#)

ECM data were smoothed with a 301 point ~~wide~~-first-order Savitsky–Golay filter (Savitsky and Golay, 1964) ~~which eliminates peaks due to random noise and small-scale variations in material chemical composition while preserving the larger peaks including those due to volcanic eruptions. As measurements were principally made in firn, we multiplied the signal by the ratio of the ice density to firn density following Kjær (2014). Finally, the ECM~~ data were normalized by subtracting the mean and dividing by the standard deviation following Karlof et al. (2000).

~~We selected potential volcanic peaks as those above the 2 $\sigma$  threshold, following standard practice (e.g. Kaczmarek et al., 2004).~~

#### 2.4. Corrections for ice flow

~~Snow burial~~The compression of snow under its own weight not only involves density changes along the vertical, but also ~~involves~~ involves lateral deformation of the underlying ice. Failure to take the latter process into account would provide an underestimation of reconstructed initial annual layer thickness, and therefore of the accumulation rate, especially within the oldest part of the record. ~~Commonly~~In this paper, ~~three~~two different models are used to represent vertical strain rate evolution with depth: (i) strain rates derived from a full Stokes model that represents the full Raymond effect measured at the ice divide (Drews et al., 2015); and (ii) a modified Dansgaard–Johnsen model (Dansgaard and Johnsen, 1969) based on the description given in Cuffey and Paterson (2000X2010).

The Drews et al. (2015) strain rate profile accounts for the best fit with the radar layers at depth, taking into account a small amount of surface thinning (0.03 m a<sup>-1</sup>) and anisotropy (although the former is not essential). From a hexagonal strain network, we calculated horizontal strain rates ( $\epsilon_{xx} + \epsilon_{yy}$ ) to be 0.002 a<sup>-1</sup>. Mass conservation then gives a vertical strain rate at the surface of -0.002 a<sup>-1</sup>. The vertical velocity profile was then scaled to match the measured vertical strain rate at the surface. A best fit to the measured radar layers was obtained with a value of a mean accumulation rate of 0.55 m a<sup>-1</sup> ice equivalent (Fig. 2).

~~From an octagonal strain network, we inferred horizontal strain rates ( $\epsilon_{xx} + \epsilon_{yy}$ ) being equal to 0.002 a<sup>-1</sup>, which from mass conservation leads to a vertical strain rate at the surface of -0.002 a<sup>-1</sup>. The vertical velocity profile was then scaled to match the measured vertical strain rate at the surface. A best fit was obtained with a value of a long-term mean accumulation rate of 0.55 m a<sup>-1</sup> ice equivalent (see Figure xx).~~

Alternatively, we used the Dansgaard–Johnsen (D–J) model to fit the characteristics at the ice divide, exhibited by the Raymond effect. Assuming that the horizontal velocity is zero, the vertical velocity is maximum at the surface and equals the accumulation rate (with negative sign) and is zero at the bed. Assuming a vertical surface strain rate of -0.002 a<sup>-1</sup>, we can determine the kink point (between constant strain rate above and a strain rate linearly

Formatted: Superscript

Formatted: Not Highlight

Formatted: Not Highlight

Formatted: Not Highlight

Formatted: Not Highlight

Formatted: Not Highlight

Formatted: Not Highlight

Formatted: Not Highlight

Formatted: Not Highlight

Formatted: Not Highlight

Formatted: Not Highlight

decreasing with depth below) that obeys these conditions (Cuffey and Paterson, 2010). This approach indicates that the kink point lies at  $0.9H$ , where  $H$  is the ice thickness. As seen in Fig. 2b, this method yields a vertical strain pattern that is consistent with that of Drews et al. (2015), especially in the first 120 m corresponding to the length of the ice core.

Formatted: Not Highlight

Formatted: Not Highlight

Formatted: Not Highlight

Formatted: Not Highlight

Formatted: Not Highlight

Formatted: Not Highlight

Formatted: Not Highlight

Formatted: Not Highlight

Formatted: Not Highlight

Formatted: Not Highlight

Formatted: Not Highlight

Formatted: Not Highlight

Formatted: Not Highlight

Formatted: Not Highlight

Formatted: Not Highlight

Formatted: Not Highlight

Both strain rates (Drews/D-J) were then used to correct the ice equivalent layer thickness for strain thinning. Layer thicknesses were then converted from ice equivalent to w.e. for easier comparison with other studies.

Alternatively, we used the Dansgaard-Johnson (D-J) model to fit the characteristics at the ice divide, exhibited by the Raymond effect. Assuming that the horizontal velocity is zero, the vertical velocity is maximum at the surface and equal to the accumulation rate (with negative sign) and is zero at the bed, and assuming a vertical surface strain rate of  $-0.002 \text{ a}^{-1}$ , we can determine the kink point that obeys these conditions (see Cuffey and Paterson). It follows that it lies at  $0.9H$ , where  $H$  is the ice thickness. As seen in Figure xx, this fits well with the strain rate profile of Drews et al. (2015). (i) a power-law model (Lliboutry, 1979), (ii) a piece-wise linear model (Dansgaard and Johnsen, 1969) and (iii) a fully linear model (Nye, 1963).

(i) The power-law model requires measurements of the borehole horizontal displacement, which are unfortunately

not available. (ii) the Nye model corrects the layer thickness  $L$  by assuming ice is incompressible, with a linear decrease from a constant annual layer thickness at the surface to zero at the ice-bedrock interface (which implies a constant total ice thickness). In that case,  $L_z = L_s(z/H)$ , where  $H$  is the total ice thickness in m w.e., and subscripts  $s$  and  $z$  represent the values at the surface and at a height  $z$  (in m w.e.) above the bed. The piece-wise model assumes a constant vertical strain rate between the surface and a given depth, which in our case is below the zone of interest since the ice core is drilled in the first quarter of the total ice rise thickness (486 m, Drews et al., 2015), and then a quadratic decrease to zero at the ice-bedrock interface. The constant strain rate in the upper part of the ice sheet can be inferred from the slope of water equivalent (w.e.) annual layer thickness versus depth, also in m w.e., assuming a constant long term snow accumulation (equal to annual layer thickness at the surface, Roberts et al., 2014). (iii) Finally, the Nye model corrects the layer thickness  $L$  by assuming ice is incompressible, with a linear decrease from a constant annual layer thickness at the surface to zero at the ice-bedrock interface (which implies a constant total ice thickness). In that case,  $L_z = L_s(z/H)$ , where  $H$  is the total ice thickness in m w.e., and subscripts  $s$  and  $z$  represent the values at the surface and at a height  $z$  (in m w.e.) above the bed.

The last two Both corrections were applied separately and are compared in the results section.

## 2.5 Community Earth System Model (CESM)

Atmospheric reanalyses and regional climate models extend back to 1979, which means that they cover only a subset of the ice core record. Instead, to interpret our ice core derived accumulation record and relate it to the large-scale climate conditions, we use output from the Community Earth System Model (CESM). To interpret our ice core derived accumulation record and relate it to the large-scale atmospheric and ocean conditions, we use outputs of the Community Earth System Model (CESM). CESM is a global, fully coupled, CMIP6-generation climate model with an approximate horizontal resolution of  $1^\circ$  degree, and has recently been used successfully to show to realistically simulate present-day Antarctic climate and SMB (Lenaerts et al., in press 2016). We use the historical time series of CESM (156 years, 1850–2005) that overlaps with most of the ice core record, and group the 16 single (~10%) years (i.e. ~10 %) with the highest accumulation and lowest accumulation in that time series. We take the mean accumulation of the ice covered CESM grid points of the coastal region around the ice core ( $20$ – $30^\circ$  East,  $69$ – $72^\circ$  South) as a representative value. For the grouped years of highest and lowest accumulation we take the anomalies (relative to the 1850–2005 mean) in near-surface temperature, and sea-ice fraction and surface pressure as parameters to describe the regional ocean and atmosphere conditions corresponding to these extreme years.

## 3 Results

### 3.1 Dating

#### 3.1.1 Relative dating (seasonal peak counting)

Figures 2–3, S1 and S2 illustrate how the high-resolution stable isotopes ( $\delta^{18}\text{O}$ ,  $\delta\text{D}$ ), smoothed ECM, chemical species and their ratios are used in combination to identify annual layer boundaries. All of these physico-chemical variables generally show a clear seasonality, undisturbed by the few very thin ice layers (white dots in Fig. 3). The summer peak in water stable isotopes is obvious in most cases. The boundary between annual layers was identified as the middle depth of the range of values of the peak above the mean  $\delta^{18}\text{O}$  value (thin black line in Fig. 3), considered as the “summer season”. Major ions Major ion such as  $\text{SO}_4^{2-}$ ,  $\text{SO}_4^{2-}/\text{Na}^+$ ,  $\text{NO}_3^-$ , and especially the ratio  $\text{Na}^+/\text{SO}_4^{2-}$  generally help to distinguish ambiguous peaks in the isotopic record.  $\text{SO}_4^{2-}$  is one of the oxidation products of Dimethyl Sulfide (DMS), a degradation product of DMSP (dimethylsulfoniopropionate) which is synthesized by sea ice microorganisms (sympagic) as an antifreeze and osmotic regulator (e.g. Levasseur, 2013). Both  $\text{nssSO}_4$  and  $\text{Na}^+/\text{SO}_4^{2-}$  vary seasonally and are also strong

Formatted: Not Superscript/ Subscript

Formatted: Not Superscript/ Subscript

Formatted: Superscript

indicators of volcanic eruptions.  $\text{NO}_3^-$  also shows a seasonal signal, but the processes controlling its seasonality are not yet fully well understood (Wolff et al., 2008). For ECM, there is also a regular seasonal signal, but only to a depth of which is sometimes blurred below 80 m, although some seasonal cycles can still be seen, for example between 115 and 118 m–80 m. (Fig. S2). The two different extreme age–depthage–depth profiles (youngest and oldest) resulting resulted from this counting procedure, taking the remaining ambiguities into account (Fig. S2). The mean age–depth profile isare presented in FigureFig. 43 with the ranges associated with the two extreme age–depth estimates. No ambiguity in layer counting is detectable above 62.38 m depth (i.e. 1933 A.D.). Between 249 237 and 269 269 annual cycles were identified between the reference surface (2012 A.D.) and the bottom of the core, which is accordinglyconsequently preliminarily provisionally dated to 17594 ± 160 A.D., before absolute dating (Sect. 3.1.2).

### 3.1.2 Absolute dating

Volcanic indicators (ECM,  $\text{nssSO}_4$ ,  $\text{SO}_4^{2-}/\text{Na}^+$ ) can be used to identify specific, dated volcanic eruptions, allowing us to reduce the uncertainties resulting from the relative dating procedure. However, unambiguous eruption identifications are challenging in ice cores from coastal regions, where the ECM and  $\text{nssSO}_4$  background signals are commonly highly variable due to the proximity of the ocean and ocean-related MSA products (Fig. S1). Given the preliminary dating of 1759 ± 16 A.D. made on the basis of our relative core dating (Section 3.1.1 above), we have looked for a specific volcanic signature with a high volcanic explosivity index (VEI) that would allow us to refine this dating in the older part of the core. The Tambora 1815 eruption, with a deposition age of 1815 ± 2 years and a VEI of 7 (Traufetter et al., 2004) has been selected. Figure 5 shows ECM along with  $\text{SO}_4^{2-}/\text{Na}^+$  and  $\text{nssSO}_4$  in the section corresponding to the age of that eruption according to our youngest and oldest estimates. The dark blue box in Fig. 5 frames the expected depth range for the “oldest estimate” while the light blue box shows the equivalent for the youngest estimate. The Tambora eruption is located at 102.35 m in the oldest estimate time scale, with an ECM signature above the 4σ threshold (twice as high as the generally used 2σ threshold (e.g. Kaczmarek et al., 2004). Further, the maximum ECM value also corresponds to a peak in  $\text{nssSO}_4$  and  $\text{SO}_4^{2-}/\text{Na}^+$  (red dotted line in Fig. 5) and, importantly, this Tambora peak occurs in wintertime (minimum  $\delta^{18}\text{O}$  value), which is opposite to where the peak would be located if it were due to the seasonal cycle. No other peak in this depth range shows high values in the three indicators. Therefore, it is very likely that our oldest estimate is closer to the real age–depth relationship than the youngest estimate. However, we will keep both of them as an evaluation of the influence of the dating uncertainty on our accumulation rates reconstruction.

Formatted: Not Highlight

Formatted: Not Highlight

Formatted: Not Highlight

Formatted: Not Highlight

Field Code Changed

Formatted: Not Superscript/ Subscript

Formatted: Not Superscript/ Subscript

Formatted: Subscript

Formatted: Not Highlight

Formatted: Not Superscript/ Subscript

In order to further improve our annual layer estimates and the depth-age relationship, we have used the ECM signal (which is mainly inherited from the  $\text{SO}_4^-$  profile) to detect volcanic eruptions using a threshold from the background signal of  $2\sigma$  (Figure 4). The best depth-age match (corresponding to the closest age match at the base of the core) was obtained with the "oldest estimate", for which 12 peaks out of 33 could be assigned to known volcanic eruptions and one more from the chemistry alone (Krakatau – 1883). Following this absolute dating recalibration, the bottom of the core is dated to 1745. The year of deposition of each volcanic peak allowed us to reduce the uncertainty of the depth-age relationship in the IC 12 core to  $\pm 2$  years. This is the precision usually associated with volcanic horizons, due to the time lapse between eruption and deposition (see sources in Table 1). The characteristics of these peaks are summarized in Table 1. The 1815 Tambora eruption has a clearly identifiable peak (Figure 4), which is expected from its high Volcanic Explosivity Index of 7 (Table 1) and its signal is detected up to two years after its eruption (e.g. Traufetter et al., 2004). Some eruptions, such as the 1762 Planchon-Peteroa eruption (assigned as unknown in Sigl et al., 2012) are recorded in both hemispheres (Sigl et al., 2012).

### 3.2 Snow accumulation rate history

Annual layer thicknesses in m w.e. for the oldest estimate: using full Stokes Drews et al. (2015) model (black line) and corrected annual layer thickness blue line, undistinguishable from the black line at this scale; using Drews et al. (2015) model with error bars (thin black line) and 11 years running mean (thick black line) for the oldest estimate; (c) same as (b) (green lines); d) Comparison of youngest (green) and oldest (black) estimates 11 years running mean. Combining the annual layer thickness data set with the continuous IC12 density profile (published in Hubbard et al., 2013), we reconstructed the accumulation rate history at the summit of Derwael-lee Risethc DIR from 17445 to 20112. The cumulative thickness in w.e. is 91.8 m (Figure 5). Without correction for layer thinning, the mean annual layer thickness is  $0.36 \pm 0.024 \pm 0.003$  m w.e., the lowest annual accumulation is  $0.14 \pm 0.05$  m w.e. in 1834 and the highest is  $1.05 \pm 0.05$  m w.e. in 1989 (Figure 6).

We applied two corrections: the modified the piece-wise linear model (Dansgaard and Johnsen model, 1969) and the adapted full Stokes model (Drews et al., 2015) the fully linear model (Nye, 1963). (see Section Sect. 4.2) to investigate the influence of ice deformation on layer thickness, both techniques assuming a constant accumulation rate and a steady state. The piece-wise model approach cannot therefore be applied to the whole data set, since plotting annual layer thickness against depth in m w.e. reveals two trends with different slopes (Figure 5), suggesting an increase in accumulation rates. The transition occurs at  $\sim 49$  m w.e., corresponding to 1900 A.D. Hypothesizing that, if accumulation rates have increased under the intensification of the hydrological cycle in response to the industrial revolution, we can consider the pre-1900 A.D. slope ( $0.003 \text{ a}^{-1}$ , Figure 5) as representative

Field Code Changed

of the rate of thinning associated with the constant long-term 'pre-industrial' rate of surface accumulation. We therefore used this strain rate value to correct annual layer thicknesses when applying the Dansgaard-Johnsen model.

Figure 6a shows the reconstructed history of annual layer thicknesses accumulation rates at IC12 from 1744.5 to 2011.2, with associated error bars without ice deformation (grey line) and with the two different ice-deformation models (modified D-J model, blue line and Drews et al., 2015, black line), which overlies each other at this scale. From now on, we will only consider the correction of Drews et al. (2015) as it is both similar and more closely guided by field measurements. As interannual variability is high, 11 years running means are also shown (thick lines in Figure 6a). As expected, the annual layer thicknesses accumulation rate without ice deformation (blue lines in Figure 6a) are underestimated in the oldest part of the ice core as relative to that with ice deformation taken compared to the other two reconstructions taking ice deformation into account. Figure 6 (b-d) shows both the oldest and the youngest estimates resulting from absolute dating to evaluate the influence of the dating uncertainty. The mean annual accumulation rate, i.e., the mean corrected annual layer thickness, is  $0.47 \pm 0.02$  m w.e. a<sup>-1</sup>. As interannual variability is high, the 11 year running means are also shown. The uncorrected curve shows a constant increase in accumulation, with multiple step-increases at 1902, 1955 and 1994 A.D. The constant increase in accumulation rates before 1902 attenuates with the correction based on the Nye approach for taking deformation into account (green lines in Figure 6a and 6b) and becomes insignificant with the Dansgaard-Johnsen model (D-J, black lines in Figure 6a and 6b). However, all curves show a clear increasing positive trend in accumulation rates since the early part of the 20<sup>th</sup> century.

Table 1 shows average annual accumulation rates for three different periods (chosen for easier comparison to with previous studies) starting from the calculated on the basis of deformation corrections (Nye and D-J) and averaged over various periods framed averaged over three different periods between by Tambora eruption and Cerro Azul volcanic horizons and the surface (1816–2011), the last 50 years compared to the previous full period of time previous (i.e., 1962–2011 cf vs. 1816–1961), and the last 20 years compared to the previous full period of time previous (i.e. 1992–2011 cf vs 1816–1992), for the youngest and oldest estimates and average between both (Table 1 (e.g. Kaczmarek et al., 2004, Sigl et al. 2012; bold years in Table 1) are shown in Figure 6b and summarized in Table 2). The long term annual accumulation, starting from the oldest volcanic layer identified: From 1768–1816 to 2011.2, the average accumulation rate is between 0.39 and  $0.46 \pm 0.02$  m w.e. a<sup>-1</sup> depending on the correction applied. For the last 50 years (Table 2). The recent (1955–2011.2), the accumulation rate is between  $0.60 \pm 0.01$  and  $0.63 \pm 0.01$  m w.e. a<sup>-1</sup> with, as expected, less impact from the different deformation corrections, representing a. The sharpest increase occurs between the periods 1902–1955 and 1955–

Formatted: Superscript

Formatted: Superscript

Formatted: Not Highlight

Formatted: Not Highlight

1992 (36% to 45% increase). With a 31-years running mean, the rate of accumulation change between 1902 and 1992 is  $0.21 \text{ m w.e. a}^{-1}$  (data not shown).  $32 \pm 4 \%$  increase compared to the period 1816–1961. For the last 20 years (1992–2011), the accumulation rate is  $0.64 \pm 0.01 \text{ m w.e. a}^{-1}$  and the increase compared to the previous record since 1816 is  $32 \pm 3 \%$ .

Formatted: Not Highlight

Formatted: Not Highlight

Formatted: Not Highlight

Table 3 shows the detailed annual accumulation rates for the last 10 years for both corrections. The highest accumulation of the last 10 years occurred in 2009 and 2011, which belong to the 3% and 1% highest accumulation years of the whole record, respectively. Table 2 shows the detailed annual accumulation rates for the last 10 years for our oldest and youngest estimates/corrections. In both estimates, the highest accumulation during the last 10 years occurred in 2009 and 2011, which belong to the 3 % and 1 % highest accumulation years of the whole record, respectively.

Formatted: Not Highlight

Formatted: English (United States), Do not check spelling or grammar

### 3.3 Sources of uncertainties

Accumulation rates reconstructed from ice cores can be characterized by substantial uncertainty show (Rupper et al., 2015). The accuracy of reconstructed snow accumulation rates depends on the dating accuracy. As discussed before/above, volcanic horizons are sometimes difficult to identify in coastal ice cores due to ECM peaks associated with the presence of marine components. We assess the influence of these uncertainties by comparing oldest and youngest estimates. Also, given our vertical sampling resolution of  $\delta^{18}\text{O}$ , the location of summer peaks is only identifiable to a precision of 0.1 m where no other data are available, but this error only affects inter-annual accumulation rates at an annual resolution, as shown by error-bars in Fig. 6. time SMB reconstructions are also influenced by density measurement error (2 % error) and small scale variability in densification. The influence on accumulation rates is very small. Callens et al. (2016) for example, used a semi-empirical model of firn compaction (Arthern et al., 2010) adjusting its parameters to fit the discrete measurements instead of using the best fit from Hubbard et al. (2013). Using the first model changes our reconstructed accumulation values by less than 2 %.

Formatted: Superscript

Formatted: Normal

Average accumulation rates on longer time periods are therefore in all cases more robust than reconstructed annual accumulation rates because they are less affected by uncertainties. These average estimates are also useful to reduce the influence of inter-annual variability.



Vertical strain rates also represent a potential source of error. A companion paper will be dedicated to a more precise assessment of this factor using repeated borehole optical televiewer stratigraphy. However, the present study uses a field-validated strain rate models which is as close as possible to reality, and shows that the using the simpler modified Dansgaard-Johnsen model changes the reconstructed accumulation rates by maximum 0.001 m w.e.. Therefore, we are confident that refining knowing the exact strain rate profile will not change our main conclusions.

Formatted: Normal

Average accumulation rates on longer time periods are therefore more robust than reconstructed annual accumulation rates because they are less affected by uncertainties. These average estimates are also useful to reduce the influence of inter-annual variability.

Uncertainties are also influenced by density measurement error 2 % and small scale variability in densification. The influence on accumulation rates is very small. Callens et al. (2016) for example, used a semi-empirical model of firm compaction (Arthern et al., 2010) adjusting its parameters to fit the discrete measurements instead of using the best fit from Hubbard et al. (2013). Using the first model changes our reconstructed accumulation values by less than 2 %. Another possible source of possible error is the potential migration of the ice divide. Indeed, radar

Formatted: Normal

layers show accumulation asymmetry next to the DIR divide, therefore, had induced non-climatic rates. However, ~~Rh~~ However, two recent analyses Drews et al (2015) found that the ice divide of the DIR must have remained laterally stable for thousands of years to explain the comparatively large Raymond arches in the ice stratigraphy. Callens et al. (2016) find a similar argument by using the radar stratigraphy in the ice-rise flanks. The possibility for an ice-divide migration is therefore small indicate that there is a very low probability that such a migration occurred as the DIR has been stable for at least the last thousands of years (Drews et al., 2015; Callens et al., 2016). Temporal variability of accumulation rates at certain locations can also be due to the presence of surface undulations up-glacier (e.g. Kaspari et al. 2004), but this effect is minimised at ice divides.

Formatted: Not Highlight

Formatted: Not Highlight

Formatted: Not Highlight

Formatted: Not Highlight

Formatted: Not Highlight

Average accumulation rates on longer time periods are therefore more robust than reconstructed annual accumulation rates because they are less affected by uncertainties. These average estimates are also useful to reduce the influence of inter-annual variability.

### 3.4.3 Relation to atmospheric and sea ice patterns Comparison with climate models

Figure 8 Figure 7 compares the trend in our IC12 SMB record with outputs from two atmospheric models: ERA-Interim reanalysis (Dee et al., 2009) and the CESM model. ERA-Interim shows no trend in the Interestingly, in the

relatively short overlapping period (1979–2012) it covers, which is not surprising since it is too short to be of climatic significance. The ice core derived SMB correlates rather poorly/moderately to ERA-Interim reanalysis (Dee et al., 2009) and RACMO2 (Lenaerts et al., 2014), yielding —(both correlation coefficient  $R^2 = 0.36$  and  $0.5–0.4$ , respectively not shown). This much poorer correlation than that compared to ice cores collected on West Antarctica (Medley et al., 2013 (GRL); Morris et al., 2015 (Nat Geo)) is presumably explained by the strong impact of local wind-induced snow redistribution and sublimation on the SMB on the wind-exposed ridge of the Derwael ice rise (Lenaerts et al., 2014). For a longer overlapping period, we used the output of the CESM model, although it is a freely evolving model that does not allow a direct comparison with measured data. The average SMB at Derwael in CESM (closest grid point) is too low ( $0.295 \pm 0.061 \text{ m a}^{-1}$ ) because the orographic precipitation effect is not well simulated with the low model resolution. Figure 8 shows the relative trends in CESM output and ERA-Interim compared to the IC12 record. However, ERA-Interim shows no trend in the short period 1979–2015 but the period is too short to explore the mechanisms. Instead, CESM does reproduce (much of) the observed trend. Subtle small-scale variations in wind speed and direction, typically not resolved by reanalyses or regional climate models, might disrupt the inter-annual variability of SMB, although we assume that it does not ~~impaenfluencet~~ the positive SMB trend found in the ice core record. Unfortunately, our method does not allow for an explicit partitioning of the SMB explained by precipitation as opposed to ~~vs.~~ wind processes. Instead, we focus on the drivers of precipitation at the ice core site using the output of CESM (Fig. 8), and we discuss it in Sect. 4.1.9). In anomalously high-accumulation years (top panel), the sea ice coverage is significantly lower than average (20–40 fewer days with sea ice cover) in the Southern Ocean northeast of the ice core location, which is the prevalent source region of the atmospheric flow (Lenaerts et al., 2013). This is associated with significantly higher near-surface temperatures (1–3 K). In low-accumulation years (not shown), we see a reverse, but less pronounced (not significant) signal, with higher sea ice fraction (10–20 days), and slightly lower temperatures and the oceanic source region of precipitation.

Figure 9. Large-scale atmospheric, ocean and sea ice anomalies in high-accumulation (10% highest) years in the CESM historical time series (1850–2005). The colours show the annual mean near-surface temperature anomaly (in °C), and the hatched areas show the anomaly in sea ice coverage (>20 days less sea ice cover than the mean). The green area shows the location of the ice core.

Figure 7 shows a summary of the output from the CESM as described in Section 2.5. In anomalously high-accumulation years (top panel), the sea ice coverage is very low (20–40 fewer days with sea ice cover) in the

Formatted: Pattern: Clear

Formatted: Pattern: Clear

Formatted: Pattern: Clear

Formatted: Superscript

Formatted: Not Highlight

Formatted: English (United Kingdom)

Field Code Changed

Southern Ocean northeast of the ice core location, which is the prevalent source region of the atmospheric flow (Lenaerts et al., 2013). This is associated with higher near-surface temperatures (1–3 K), and a strengthening of the low-climatological low-pressure system (>1 hPa lower surface pressure), located offshore the ice core location (Lenaerts et al., 2013). In low-accumulation years (bottom panel), we see a reverse, albeit less strong, signal, with higher sea ice fraction, lower temperatures and higher core pressure of the low-pressure system.

## 4 Discussion

### 4.1 Regional-scaleSmall-scale variability

Figure 9. Large-scale atmospheric, ocean and sea-ice anomalies in high-accumulation (10% highest) years in the CESM historical time series (1850–2005). The colours show the annual mean near-surface temperature anomaly (in °C), and the hatched areas show the anomaly in sea-ice coverage (>20 days less sea ice cover than the mean). The green area shows the location of the ice core.

Small scale spatial variability in cyclonic activity and atmospheric rivers could both explain why our results are different from others in the same region, and why they correlate only moderately to the climate reanalyses (ERA-Interim and RACMO2). Orography can greatly affect spatial variability in SMBsnow-accumulation (Lenaerts et al., 2014). Local wind phenomena are important factors of interannual variability. Indeed, the lower correlation with ERA-Interim and RACMO2 in our study, as compared to ice cores collected on West Antarctica (Medley et al., 2013; MorrisThomas et al., 2015) is presumably explained by the strong influence of local wind-induced snow redistribution and sublimation on the SMB on the wind-exposed ridge of the Derwael-ice riseDIR (Lenaerts et al., 2014).

However, Callens et al. (2016) showed that this spatial pattern has been constant for the last thousands of years. Therefore, the observed trend of increasing annual accumulation is highly unlikely to be explained by a different orographic precipitation pattern caused by a change in local wind direction or strength, which would cause a different orographic precipitation pattern. This argument, along with the existing correlations with ERA-Interim and RACMO2, suggests that these trends are not only representative of the climate on the DIR-the Roi-Baudouin ice shelf but that they are also representative of at least the Roi Baudouin ice shelf, surrounding the DIR typical of a wider area.

Formatted: Not Highlight

Formatted: Not Highlight

Formatted: Pattern: Clear

Formatted: Not Highlight

Formatted: Not Highlight

Formatted: Not Highlight

Formatted: Not Highlight

Formatted: Not Highlight

Formatted: Not Highlight

Formatted: Not Highlight

The output of the CESM (Figure 9) can be used as a preliminary indicator of the drivers of precipitation at the ice core location. In anomalously high accumulation years, the sea ice coverage is substantially lower than average (20–40 fewer days with sea-ice cover) in the Southern Ocean northeast of the ice core location, which is the prevalent source region of the atmospheric flow to the DIR (Lenaerts et al., 2013). This is associated with considerably higher near-surface temperatures (1–3 K). In low-accumulation years (not shown), we see a reverse, but less pronounced (not significant) signal, with higher sea ice fraction (10–20 days), and slightly lower temperatures and the oceanic source region of precipitation.

#### 4.2.1 Spatial and temporal Continental-scale variability

Our results show an increase in accumulation on the Derwael Ice Rise in coastal DML from 1955 onward during the 20<sup>th</sup> and 21<sup>st</sup> centuries. This confirms the studies that show a current recent increase in precipitation in coastal East Antarctica on the basis of satellite data and regional climate models (Davis et al., 2005, Lenaerts et al., 2012). Using a new glacial isostatic adjustment model, King et al. (2012) estimated that a  $60 \pm 13$  Gt a<sup>-1</sup> mass increase for the East Antarctic Ice Sheet during the most recent period last 20 years was concentrated along coastal regions, particularly in DML. However, until now, no change had been detected in ice cores from the area. Our study is the first in situ validation of an climate-related increase in coastal Antarctic precipitation, which is expected to occur mainly in the peripheral areas at surface elevations below 2250 m (Krinner et al., 2007; Genthon et al., 2009).

However, not all of Antarctica would be expected to have the same accumulation trend. Figure 1 and Table A1 summarize results on accumulation trends from previous studies based on ice cores, extended with a few studies based on stake networks and radar. The colours of the sites position indicated on Figure 1 refers to show the accumulation change at that site. The reference period refers to corresponds to the last ~200 years, the recent period and it was compared to two recent periods of different lengths, corresponding approximately to the last ~50 years and to the most recent period to the last ~20 years. The exact periods are given in Table A1.

Although the ISMASS Committee (2004) pointed out the importance of analysing coastal records, only 25 of the temporal records found in the literature concern ice cores drilled at less than 100 km from the coast and below 1500 m above sea level, and only 16 of them are located in DML. Only two of those records cover a period longer than 20–100 years: S100 (Kaczmarek et al., 2004) and B04 (Schlosser and Oerter, 2002). They both show a small decreasing negative trend (Figure 1).

Formatted: Superscript

Formatted: Superscript

For the whole continent, most studies (69 % of those comparing the last ~50 years with the last ~200 years) show no lack a significant trend (< 10 % change). When we consider only the studies comparing the last 20 years to the last 200 years, the percentage reporting no significant trend falls from 69 % to 46 %, for all Antarctica, but the trends revealed are both positive and negative. For example, Isaksson et al. (1996) found < 3 % change at the EPICA drilling site (Amundsenisen, DML) between 1865-1965 and 1966–1991. No trend was found on most inland and coastal sites (e.g. B31, S20) in DML, for the second part of the 20<sup>th</sup> century (Isaksson et al., 1999; Oerter et al. 1999, 2000; Hofstede et al., 2004; ) or for the recent period (Fernandoy et al., 2010). When we consider only the studies comparing the last 20 years to the last 200 years, the percentage reporting no significant trend falls from 69 % to 46 %. The trends revealed are both positive and negative and concern the whole Antarctic continent.

A few studies (9% for the larger period and 18% for the shorter, more recent period) show a decrease of more than 10 % (9 % of the studies observed this decrease during for the last ~50 years and 18 % during for the last ~20 years). This is the case for several inland sites in DML (e.g. Anschutz et al., 2011), but also coastal sites in this region (Kaczmarek et al., 2004; S100; Isaksson & Melvold, 2002; Site H; Isaksson et al., 1999; S20; Isaksson et al., 1996; Site E; Isaksson et al., 1999; Site M).

Twenty-one percent of the studies record an increase of > 10 % of accumulation rates starting during the last ~50 years from the middle of the 20<sup>th</sup> century, and 36 % of the studies show such an increase during the most recent period starting during the last ~20 years. In East Antarctica, increasing positive trends were only recorded at inland sites, e.g. in DML (Moore et al., 1991; Oerter et al., 2000), at South Pole Station (Mosley & Thompson, 1999), Dome C (Frezzotti et al., 2005), and around Dome A (Ren et al., 2010; Ding et al., 2011). Other increasing positive trends were found on the Antarctic Peninsula in coastal West Antarctica (Thomas et al., 2008; Aristarain et al., 2004). For some sites, the increase only started during the last ~20 years ago the most recent period (Site M: Karlof et al., 2005). The only other coastal site in East Antarctica potentially showing an increase in snow accumulation rates is Talos Dome, where Frezzotti et al. (2013) reported a 19% decrease during the period 1966-1996 (compared to 1816-2001), while Stenni et al. (2002) reported an increase by 11% during 1992-1996 (compared to 1816-1996).

Following Frezzotti et al. (2013), a pattern arises when we compare the low accumulation sites with to the high accumulation sites (not all coastal), setting the threshold at 0.3 m w.e. a<sup>-1</sup>, following Frezzotti et al. (2013) (Figure Fig. 810). The 11 sites above 0.3 m w.e. a<sup>-1</sup> show an average increase in accumulation of 34.3 3.8% between the last ~50 years and the reference period (last ~200 years), whereas the sites with lower accumulation show no trend (Figure Fig. 8a10a). This increase is would be more important (75%) if we compare the same

Formatted: Pattern: Clear

Formatted: Font color: Auto, English (United Kingdom)

Formatted: Not Highlight

reference period with the ~~most recent period~~ (last ~20 years) but this ~~only covers~~ is covered by only two high accumulation sites, including IC12 (Figure Fig. 98b). Comparing the ~~most recent period last ~20 years with~~ the last ~50 years, the 12 high accumulation sites show an average increase of ~~9.9~~ 40.1% (Figure Fig. 98c).

#### 4.2 Sources of uncertainties

5 It is important to keep in mind that the trends, reported in this study (and others) have considerable uncertainties (Rupper et al., 2015). The accuracy of reconstruction of past snow accumulation rates depends on the dating exactness. Volcanic horizons are sometimes difficult to identify in coastal ice cores due to the ECM peaks associated with the presence of marine components. Also, given our vertical sampling resolution, the location of any single summer peak is only identifiable to a precision of 0.1 m. However, annual layer counting is easier than  
10 on inland sites, due to higher accumulation rates. Average accumulation rates on longer periods are preferred, since they are less affected by uncertainties than annual accumulation rates. These average estimates are also useful to reduce the influence of inter-annual variability.

Vertical strain rates are also a potential source of error. A companion paper will be dedicated to a more precise assessment of this factor using repeated borehole optical televiewer stratigraphy. However, the present study, by  
15 using a range of available strain rate models, shows that knowing the exact strain rates should not affect our main conclusions. Uncertainties are also influenced by the error on density and small scale variability in densification but these are assumed to be very small. For example, Callens et al. (submitted) used a semi-empirical model of firn compaction (Arthern et al., 2010) adjusting its parameters to fit the discrete measurements instead of using the best fit in Hubbard et al. (2013). Using the first model changes accumulation values by less than 2% (data not  
20 shown). Another source of possible error is the potential migration of the ice divide. Indeed, radar layers show accumulation asymmetry next to the Derwael ice Rise divide; if the divide migrated, it could have affected the change in accumulation. However, recent data indicate that there is a very low probability that such a migration occurred (Drews et al., 2015). Temporal variability at certain locations can also be due to the presence of surface undulations up glacier (e.g. Kaspari et al., 2004), but this is not the case for ice divides.

#### 25 4.3.3 Causes of spatial and temporal variability

The ~~increasing positive~~ temporal trend in ~~snow accumulation~~ SMB measured here and in ice cores from other areas, ~~as well as the apparent and the observed~~ spatial contrast, ~~observed~~ could be the result of ~~variable forcing~~: thermodynamic ~~forcing~~ (temperature change), dynamic ~~forcing~~ (change in atmospheric circulation) or both.

~~Increasing-Higher~~ temperature ~~increases-induces~~ higher saturation vapor pressure~~the capacity of the air to hold vapour~~, generally enhancing precipitation. Oerter et al., (2000) ~~demonstrateshowed~~ a correlation between temperature and accumulation rates in DML. On longer timescales (~~glacial-interglacial~~), using ice cores and models, Frieler et al., (2015) found a correlation between temperature and accumulation rates for the whole Antarctic continent. However, Altnau et al. (2015) found no correlation between snow accumulation and changes in ice  $\delta^{18}\text{O}$  in coastal cores. They hypothesized that changes in synoptic circulation (cyclonic activity) have more influence at the coast than thermodynamics~~-alone~~.

~~In the presence of a blocking anticyclone at subpolar latitudes, an amplified Rossby wave invokes the advection of~~  
~~The increased frequency of blocking anticyclone and amplifying Rossby waves leads to the advection of moist~~  
~~air from the warmer middle and low latitudes~~ (Schlosser et al., 2010; Frezzotti et al., 2013). Meridional moisture transport towards DML is sometimes concentrated into “atmospheric rivers” of which two recent manifestations, in 2009 and 2011, have led to a recent positive mass balance of the East Antarctic ice sheet (Shepherd et al., 2012; Boening et al., 2012). It was also observed in situ, at a local scale, next to the Belgian Princess Elisabeth base (72°S, 21°E) (Gorodetskaya et al., 2013; 2014). Several of these~~Multiple of these-~~ precipitation events in a single year can represent up to 50 % of the annual accumulation ~~further~~ away from the coast (Schlosser et al., 2010; Lenaerts et al., 2013). However, these two years are also observed in our data as two notably higher than average accumulation years (2009 and 2011, Table 32).~~This moisture transport is sometimes concentrated into “atmospheric rivers” of which two recent manifestations, in 2009 and 2011, have led to a positive anomaly in the net mass balance of East Antarctica (Shepherd et al., 2012; Boening et al., 2012) which was also observed in situ, at a local scale, next to the Belgian Princess Elisabeth base (72°S, 21°E) (Gorodetskaya et al., 2013; 2014). Such individual precipitation events can represent up to 50% of the annual accumulation (Schlosser et al., 2010; Lenaerts et al., 2013). These two highly variable accumulation events are also observed in our data as two notably higher than average accumulation years (2009 and 2011, Table 3). Our record puts places these extreme events within an historical perspective. Despite the fact that higher accumulation years exist in the recent part of record, confirming that they 2009 and 2010 are amongst the 1 % to 3 % highest accumulation years of the last two centuries. despite the fact that higher accumulation years exist in the recent part of record.~~

A change in climate modes could also partly explain recent changes in accumulation. The Southern Annular Mode (SAM) has shifted to a more positive phase during the last 50 years (Marshall, 2003). This has led to increasing cyclonic activity, but also increasing wind speed and sublimation. Kaspari et al. (2004) also established a link between periods of increased accumulation and sustained El Niño events (negative Southern Oscillation Index (SOI) anomalies) in 1991–95 and 1940–42. ~~We compared our detrended data set with SOI and SAM time series~~

Formatted: Not Highlight

(KNMI, 2015) and found no correlation with either of those two indexes, yielding respective  $R^2$  value of 0.0016 and 0.0026. In our detrended dataset (not shown), mean accumulation is indeed 5 % higher during 1991–95 than the long-term average and 17 % higher during 1940–42. However, high accumulation is also recorded during 1973–75 (19 % higher than average) while that period is characterized by positive SOI values. Therefore, climate modes seem to have little influence (or an influence of unconstrained complexity) on inter-annual variability of accumulation rates at IC12.

Highest snowfall and highest trends in predicted snowfall are expected in the escarpment zone of the continent, due to orographic uplift (Genthon et al., 2009). The main factor generating spatial and interannual variability is the wind, and wind ablation represents one of the largest sources of uncertainty in modelling SMB. Highest snowfall and highest trends in predicted snowfall are expected in the escarpment zone of the continent, due to orographic uplift (Genthon et al., 2009). For example, in the escarpment area of DML, low and medium precipitation amounts can be entirely removed by the wind, while high precipitation events lead to net accumulation (Gorodetskaya et al., 2015). An increase in accumulation coupled with an enhanced wind speed could result in increased SMB where the wind speed is low and decreased SMB in the windier areas (90 % of the Antarctic surface, Frezzotti et al., 2004). Frezzotti et al. (2013) suggested that snow accumulation has increased at low altitude sites and on the highest ridges due to more frequent anticyclonic blocking events, but has decreased at intermediate altitudes due to stronger wind ablation in the escarpment areas. In DML, however, Altnau et al. (2015) reported an accumulation increase on the plateau (coupled to an increase in  $\delta^{18}\text{O}$ ) and a decrease on coastal sites, which they associated with a change in circulation patterns. Around Dome A, Ding et al. (2011) also reported an increase in accumulation in the inland area and a recent decrease towards the coast. Their explanation is that air masses may transfer moisture inland more easily due to climate warming. A combination of the wind spatial variability and the local nature of the atmospheric phenomenon potentially involved can explain the spatially contrasting trends observed.

A more recent study using a fully coupled climate model (Lenaerts et al., 2016) suggests that DML is the region most susceptible to an increase in snowfall in a present and future warmer climate. The snowfall increase in the coastal regions is particularly attributed to loss of sea ice cover in the Southern Atlantic Ocean, which in turn enhances atmospheric moisture uptake by evaporation. This is further illustrated in Fig. 8, which suggests that extremely high accumulation years are associated with low sea ice cover. The longer exposure of open water leads to higher near-surface temperatures and enhances evaporation and moisture availability for ice sheet precipitation (Lenaerts et al., 2016).

Formatted: Not Highlight

Formatted: Not Highlight

Formatted: Not Highlight



Small-scale spatial variability in cyclonic activity and atmospheric rivers could explain why our results are different from others in the same region. Orography can greatly affect spatial variability in snow accumulation (Lenaerts et al., 2013). Highest snowfall and highest trends in predicted snowfall are expected in the escarpment zone, due to orographic uplift (Genthon et al., 2009). The main factor generating spatial variability, however, is commonly the wind; wind ablation represents one of the largest sources of uncertainty in modelling SMB. For example, in the escarpment area of DML, low and medium precipitation amounts can be entirely removed by the wind, while high precipitation events lead to net accumulation (Gorodetskaya et al., 2015). An enhanced wind speed coupled with an increase in accumulation could only increase SMB where the wind speed is low, while decreasing SMB in the windier areas (90% of the Antarctic surface (Frezzotti et al., 2004)). Frezzotti et al. (2013) suggested that snow accumulation has increased at low altitude sites and on the highest ridges due to more frequent anticyclonic blocking events, but has decreased at intermediate altitudes due to stronger wind ablation in the escarpment areas. In DML however, Altnau et al. (2015) reported an accumulation increase on the plateau (coupled to an increase in  $\delta^{18}\text{O}$ ) and a decrease on coastal sites, which they associated with a change in circulation patterns. Around Dome A, Ding et al. (2011) also reported an increase in accumulation rate in the inland area and a recent decrease towards the coast. Their explanation is that air masses may transfer moisture inland more easily due to climate warming. A more recent study using a fully coupled climate model (Lenaerts et al., in press) suggests that DML is the region most susceptible to an increase in snowfall in a present and future warmer climate. The snowfall increase in the coastal regions is particularly attributed to loss of sea ice cover in the Southern Atlantic Ocean, which in turn enhances atmospheric moisture uptake by evaporation. This is further illustrated in Figure 7, which shows that extremely high accumulation years are associated with low sea ice cover. The longer exposure of open water leads to higher near-surface temperatures and enhances evaporation and moisture availability for ice sheet precipitation (Lenaerts et al., in press). Additionally, the low pressure system, located offshore the ice core location (Lenaerts et al., 2013) is strengthened and invigorates meridional heat and moisture transport towards the ice sheet. The opposite is true for extremely low accumulation years.

## 5 Conclusions

A 120 m ice core was drilled on the divide of the DIRerwael ice rise, and dated back to  $1759 \pm 16$  A.D.  $1745 \pm 2$  A.D. using  $\delta^{18}\text{O}$ ,  $\delta\text{D}$ , major ions, major ion where necessary, and volcanic horizons identified from ECM data. Three volcanic indicators allowed the identification of Tambora 1820 eruption, which constrained the dating of the bottom of the ice core to  $1743 \pm 2$  A.D. to the oldest estimate. However, we take into account the unconstrained

Formatted: Pattern: Clear (Yellow)

dating uncertainty to calculate the mean-average accumulation and temporal trends at this site. The average accumulation between 1816–2011 is  $0.47 \pm 0.020$   $\pm 0.035$  m w.e. a<sup>-1</sup> after corrections for densification and dynamic layer thinning. An increasing trend  $32 \pm 4$  % increase in accumulation rate is reconstructed-observed from 1955 onwards during the 20<sup>th</sup> and 21<sup>st</sup> centuries, confirming the relative trend calculated by the CESM for this area, as expected from climate models. Wind redistribution may well have a substantial impact on interannual variability of accumulation rates at the DIR, but it is unlikely that it has an influence on the temporal trend.

The trends in accumulation observed in other records all over Antarctica are spatially highly variable. In coastal East Antarctica, our study is the only to show an increase in accumulation during the 20<sup>th</sup> and 21<sup>st</sup> centuries. Many studies point to a difference in the behaviour of coastal and inland sites, due to a combination of thermodynamics and dynamic processes. A combination of spatial variability in snowfall and snow redistribution by the wind explain the observed spatial variations and the poor correlation between our record and the climate reanalyses (ERA-Interim and RACMO2). A combination of the wind spatial variability and the local nature of the atmospheric phenomenon potentially involved can explain the spatially contrasting trends observed. Spatial variability in wind patterns, cyclonic activity and atmospheric rivers could explain why our results are different from others in the same region, and why they correlate only moderately to the climate reanalyses (ERA-Interim and RACMO2). Our results of the analysis based on CESM output suggests that accumulation variability is also potentially largely explained by changes in sea ice cover combined with regional atmospheric changes, and atmospheric patterns. More studies are, however still clearly needed at other coastal sites in East Antarctica to determine how representative this result is.

Long time-series of annual accumulation rates are scarce in coastal East Antarctica. The divide of Derwael Ice Rise is a suitable drilling site for deep drilling. It has a high accumulation rate, and appropriate ice conditions (few thin ice layers) for paleoclimate reconstruction. With a 486 m ice thickness, drilling to the bedrock could reveal at least 2000 years of a reliable climate record with high resolution, a priority target of the International Partnership in Ice Core Science (IPICS, Steig et al., 2005). The divide of Derwael Ice Rise is a suitable drilling site for deep drilling. It has a high accumulation rate, and appropriate ice conditions (few thin ice layers) for paleoclimate reconstruction. According to the full Stokes model (Drews et al., 2015), drilling to 350 m could reveal at least 2000 years of a reliable climate record with high resolution, which would address one of the priority targets ("IPICS-2k array", Steig et al., 2005) of the International Partnership in Ice Core Science (IPICS).

Formatted: Not Highlight

Formatted: Superscript

## Data Availability

~~Age-depth~~Age-depth data and uncorrected accumulation rates are available online (doi:10.1594/PANGAEA.857574).

## 5 Acknowledgements

This paper forms a contribution to the Belgian Research Programme on the Antarctic (Belgian Federal Science Policy Office), Project SD/SA/06A Constraining ice mass changes in Antarctica (IceCon). The authors wish to thank the International Polar Foundation for logistic support in the field. MP is partly funded by a grant from Fonds David et Alice Van Buuren. JTML is funded by Utrecht University through its strategic theme Sustainability, sub-theme Water, Climate & Ecosystems, and the programme of the Netherlands Earth System Science Centre (NESSC), financially supported by the Ministry of Education, Culture and Science (OCW). Ph. C. thanks the Hercules Foundation ([www.herculesstichting.be/](http://www.herculesstichting.be/)) for financing the upgrade of the stable isotope laboratory. The research leading to these results has received funding from the European Research Council under the European Community's Seventh Framework Programme (FP7/2007-2013) / ERC grant agreement 610055 as part of the Ice2Ice project. The authors also thank Irina Gorodetskaya for her helpful comments. [The initial version of the manuscript has benefited from the very constructive comments and corrections of two anonymous referees.](#)

## References

- Altnau, S., Schlosser, E., Isaksson, E., & Divine, D.: Climatic signals from 76 shallow firn cores in Dronning Maud Land, East Antarctica, *The Cryosphere*, 9(3), 925-944, 2015.
- 20 Anschütz, H., Müller K., Isaksson, E., McConnell, J. R., Fischer, H., Miller, H., Albert, M., and Winther, J.-G.: Revisiting sites of the South Pole Queen Maud Land Traverses in East Antarctica: accumulation data from shallow firn cores, *J. Geophys. Res.*, 114, D24106, doi:10.1029/2009JD012204, 2009.
- Anschütz, H., Sinisalo, A., Isaksson, E., McConnell, J. R., Hamran, S.-E., Bisiaux, M. M., Pasteris, D., Neumann, T. A., and Winther, J.-G.: Variation of accumulation rates over the last eight centuries on the East Antarctic Plateau derived from volcanic signals in ice cores, *J. Geophys. Res.*, 116, D20103, doi:10.1029/2011JD015753, 2011.
- 25

Formatted: Indent: Left: 0", Hanging: 0.5"

- Arthern, R. J., Vaughan, D. G., Rankin, A. M., Mulvaney, R., and Thomas, E. R.: In situ measurements of Antarctic snow compaction compared with predictions of models, *J. Geophys. Res.*, 115, F03011, doi:10.1029/2009JF001306, 2010.
- Aristarain, A. J., Delmas, R. J., and Stievenard, M.: Ice-core study of the link between sea-salt aerosol, sea-ice cover and climate in the Antarctic Peninsula area, *Clim. Change*, 67, 63–86, 2004.
- Boening, C., Lebedev, M., Landerer, F., and Stephens, G.: Snowfall driven mass change on the East Antarctic ice sheet, *Geophys. Res. Lett.*, 39, L21501, doi:10.1029/2012GL053316, 2012.
- Bromwich, D. H., Nicolas, J. P., and Monaghan, A. J.: An assessment of precipitation changes over Antarctica and the Southern Ocean since 1989 in contemporary global reanalyses, *J. Clim.*, 24, 4189–4209, 2011.
- 10 [Bromwich, D. H., Nicolas, J. P., Monaghan, A. J., Lazzara, M. A., Keller, L. M., Weidner, G. A., and Wilson, A. B.: Corrigendum: Central West Antarctica among the most rapidly warming regions on Earth. \*Nature Geoscience\*, 7\(1\), 76–76, 2014.](#)
- Callens, D., Drews, R., Witrant, E., Philippe, M., and Pattyn, F.: [Temporally stable surface mass balance asymmetry across an ice rise derived from radar internal reflection horizons through inverse modeling](#)~~Surface mass balance anomaly across an ice rise derived from internal reflection horizons through inverse modelling~~, *J. Glaciol.*, *in press*, doi:10.1017/jog.2016.41, 2016.
- 15 [Cuffey, K. M., and Paterson, W.: The physics of glaciers, Elsevier, 693 pp., 2010.](#)
- Dansgaard, W., and Johnsen, S.: A flow model and a time scale for the ice core from Camp Century, Greenland, *J. Glaciol.*, 8, 215–223, 1969.
- 20 Davis, C. H., Li, Y., McConnell, J. R., Frey, M. M., and Hanna, E.: Snowfall-driven growth in East Antarctic Ice Sheet mitigates recent sea-level rise, *Science*, 308, 1898–1901, 2005.
- Ding, M., Xiao, C., Li, Y., Ren, J., Hou, S., Jin, B., and Sun, B.: Spatial variability of surface mass balance along a traverse route from Zhongshan station to Dome A, Antarctica, *J. Glaciol.*, 57, 658–666, doi:10.3189/002214311797409820, 2011.
- 25 [Drews, R., Martin, C., Steinhage, D., & Eisen, O.: Characterizing the glaciological conditions at Halvfarryggen ice dome, Dronning Maud Land, Antarctica. \*J. Glaciol.\*, 59\(213\), 9–20, 2013.](#)
- Drews, R., Matsuoka, K., Martin, C., Callens, D., Bergeot, N., and Pattyn, F.: Evolution of Derwael Ice Rise in Dronning Maud Land, Antarctica, over the last millennia, *J. Geophys. Res., Earth Surf.*, 120, 564–579, doi: 10.1002/2014JF003246, 2015.

Formatted: Not Highlight

- Ekaykin, A. A., Lipenkov, V. Y., Kuzmina, I., Petit, J. R., Masson-Delmotte, V., and Johnsen, S. J.: The changes in isotope composition and accumulation of snow at Vostok station, East Antarctica, over the past 200 years, *Ann. Glaciol.*, 39, 569–575, 2004.
- Fernandoy, F., Meyer, H., Oerter, H., Wilhelms, F., Graf, W., and Schwander, J.: Temporal and spatial variation of stable-isotope ratios and accumulation rates in the hinterland of Neumayer station, East Antarctica, *J. Glaciol.*, 56, 673–687, 2010.
- Frezzotti, M., Pourchet, M., Flora, O., Gandolfi, S., Gay, M., Urbini, S., Vincent, C., Becagli, S., Gragnani, R., Proposito, M., Severi, M., Traversi, R., Udisti, R., and Fily, M.: New estimations of precipitation and surface sublimation in East Antarctica from snow accumulation measurements, *Clim. Dyn.*, 23, 803–813, doi:10.1007/s00382-00004-00462-0038500803-00813, 2004.
- Frezzotti, M., Pourchet, M., Flora, O., Gandolfi, S., Gay, M., Urbini, S., Vincent, C., Becagli, S., Gragnani, R., Proposito, M., Severi, M., Traversi, R., Udisti, R., and Fily, M.: Spatial and temporal variability of snow accumulation in East Antarctica from traverse data, *J. Glaciol.*, 51, 113–124, 2005.
- Frezzotti, M., Urbini, S., Proposito, M., Scarchilli, C., and Gandolfi, S.: Spatial and temporal variability of surface mass balance near Talos Dome, East Antarctica, *J. Geophys. Res.*, 112, F02032, doi:10.1029/2006JF000638, 2007.
- Frezzotti, M., Scarchilli, C., Becagli, S., Proposito, M., and Urbini, S.: A synthesis of the Antarctic surface mass balance during the last 800 yr, *The Cryosphere*, 7, 303–319, doi: 10.5194/tc-7-303-2013, 2013.
- Frieler, K., Clark, P. U., He, F., Buizert, C., Reese, R., Ligtenberg, S. R., van den Broeke, M. R., Winkelmann, R., and Levermann, A.: Consistent evidence of increasing Antarctic accumulation with warming, *Nat. Clim. Change*, 5, 348–352, doi: 10.1038/nclimate2574, 2015.
- Fujita, S., Holmlund, P., Andersson, I., Brown, I., Enomoto, H., Fujii, Y., Fujita, K., Fukui, K., Furukawa, T., Hansson, M., Hara, K., Hoshina, Y., Igarashi, M., Iizuka, Y., Imura, S., Ingvander, S., Karlin, T., Motoyama, H., Nakazawa, F., Oerter, H., Sjöberg, L. E., Sugiyama, S., Surdyk, S., Ström, J., Uemura, R., and Wilhelms, F.: Spatial and temporal variability of snow accumulation rate on the East Antarctic ice divide between Dome Fuji and EPICA DML, *The Cryosphere*, 5, 1057–1081, doi:10.5194/tc-5-1057-2011, 2011.
- Genthon, C., Krinner, G., and Castebrunet, H.: Antarctic precipitation and climate-change predictions: horizontal resolution and margin vs plateau issues, *Ann. Glaciol. Annals of Glaciology*, 50(50), 55–60, 2009.
- Gorodetskaya, I. V., Van Lipzig, N. P. M., Van den Broeke, M. R., Mangold, A., Boot, W., and Reijmer, C. H.: Meteorological regimes and accumulation patterns at Utsteinen, Dronning Maud Land, East Antarctica:

Formatted: English (United States)

Formatted: English (United States)

Formatted: English (United States)

Formatted: English (United States)

Formatted: English (United States)

Analysis of two contrasting years, *J. Geophys. Res.-Atmos.*, 118, 1700–1715, doi:10.1002/jgrd.50177, 2013.

Gorodetskaya, I. V., Tsukernik, M., Claes, K., Ralph, M. F., Neff, W. D., and Van Lipzig, N. P. M.: The role of atmospheric rivers in anomalous snow accumulation in East Antarctica, *Geophys. Res. Lett.*, 41, 6199–6206, doi:10.1002/2014GL060881, 2014.

Gorodetskaya, I. V., Kneifel, S., Maahn, M., Van Tricht, K., Thiery, W., Schween, J. H., Mangold, A., Crewell, S., and Van Lipzig, N. P. M.: Cloud and precipitation properties from ground-based remote-sensing instruments in East Antarctica, *The Cryosphere*, 9(4), 285–304, doi:10.5194/tc-9-285-2015, 2015.

Hammer, C.U.: Acidity of polar ice cores in relation to absolute dating, past volcanism, and radio-echoes, *J. Glaciol.*, 25(93), 359–372, 1980.

Hammer, C. U., Clausen, H. B., and Langway Jr, C. C.: Electrical conductivity method (ECM) stratigraphic dating of the Byrd Station ice core, Antarctica, *Annals Ann. of Glaciology*, 20, 115–120, 1994.

Hofstede, C. M., van de Wal, R. S. W., Kaspers, K. A., van den Broeke, M. R., Karlöf, L., Winther, J. G., Isaksson, E., Lappégard, G., Mulvaney, R., Oerther, H., and Wilhelms, F.: Firm accumulation records for the past 1000 years on the basis of dielectric profiling of six firm cores from Dronning Maud Land, Antarctica, *J. Glaciol.*, 50, 279–291, 2004.

Hubbard, B., Roberson, S., Samyn, D., and Merton-Lyn, D.: Digital optical televising of ice boreholes, *J. Glaciol. Journal of Glaciology*, 54(188), 823–830, 2008.

Hubbard, B., Tison, J.-L., Philippe, M., Heene, B., Pattyn, F., Malone, T., and Freitag, J. J.: Ice shelf density reconstructed from optical televiewer borehole logging, *Geophys. Res. Lett.*, 40(22), 5882–5887, 2013.

Igarashi, M., Nakai, Y., Motizuki, Y., Takahashi, K., Motoyama, H., and Makishima, K.: Dating of the Dome Fuji shallow ice core based on a record of volcanic eruptions from AD 1260 to AD 2001, *Polar Sci.*, 5, 411–420, doi:10.1016/j.polar.2011.08.001, 2011.

Isaksson, E., and Melvold, K.: Trends and patterns in the recent accumulation and oxygen isotope in coastal Dronning Maud Land, Antarctica: interpretations from shallow ice cores, *Ann. Glaciol.*, 35, 175–180, 2002.

Isaksson, E., Karlén, W., Gundestrup, N., Mayewski, P., Whitlow, S., and Twickler, M.: A century of accumulation and temperature changes in Dronning Maud Land, Antarctica, *J. Geophys. Res.*, 101, 7085–7094, 1996.

Isaksson, E., van den Broeke, M. R., Winther, J.-G., Karlöf, L., Pinglot, J. F., and Gundestrup, N.: Accumulation and proxytemperature variability in Dronning Maud Land, Antarctica, determined from shallow firm cores, *Ann. Glaciol.*, 29, 17–22, 1999.

- ISMASS Committee: Recommendations for the collection and synthesis of Antarctic Ice Sheet mass balance data, *Global Planet. Change*, 42, 1–15, doi:10.1016/j.gloplacha.2003.11.008, 2004.
- Jiang, S., Cole-Dai, J., Li, Y., Ferris, D.G., Ma, H., An, C., Shi, G., and Sun, B.: A detailed 2840 year record of explosive volcanism in a shallow ice core from Dome A, East Antarctica, *J. Glaciol.*, 58, 65–75, doi:10.3189/2012JoG11J138, 2012.
- Kaczmarek, M., Isaksson, E., Karlöf, K., Winther, J.-G., Kohler, J., Godtliebsen, F., Ringstad Olsen, L., Hofstede, C. M., van den Broeke, M. R., Van DeWal, R. S.W., and Gundestrup, N.: Accumulation variability derived from an ice core from coastal Dronning Maud Land, Antarctica, *Ann. Glaciol.*, 39, 339–345, 2004.
- 10 Karlöf, L., Winther, J. G., Isaksson, E., Kohler, J., Pinglot, J. F., Wilhelms, F., Hansson, M., Holmlund, P., Nyman, M., Pettersson, R., Stenberg, M., Thomassen, M. P. A., van der Veen, C., and van de Wal, R. S. W., & Wal, R. V. D.: A 1500 year record of accumulation at Amundsenisen western Dronning Maud Land, Antarctica, derived from electrical and radioactive measurements on a 120 m ice core, *J. Geophys. Res.: Atmospheres* (1984–2012), 105(D10), 12471–12483, doi:10.1029/1999JD901119, 2000.
- 15 Karlöf, L., Isaksson, E., Winther, J. G., Gundestrup, N., Meijer, H. A. J., Mulvaney, R., Pourcher, M., Hofstede, C., Lappégard, G., Pettersson, R., van den Broeke, M. R., and van de Wal, R. S. W.: Accumulation variability over a small area in east Dronning Maud Land, Antarctica, as determined from shallow firn cores and snow pits: some implications for ice, *J. Glaciol.*, 51, 343–352, doi:10.3189/172756505781829232, 2005.
- Kaspari, S., Mayewski, P. A., Dixon, D. A., Spikes, V. B., Sneed, S. B., Handley, M. J., and Hamilton, G. S.: Climate variability in west Antarctica derived from annual accumulation-rate records from ITASE firn/ice cores, *Ann. Glaciol.*, 39, 585–594, doi:10.3189/172756404781814447, 2004.
- 20 King, M. A., Bingham, R. J., Moore, P., Whitehouse, P. L., Bentley, M. J., and Milne, G. A.: Lower satellite-gravimetry estimates of Antarctic sea-level contribution, *Nature*, 491, 586–589, doi:10.1038/nature11621, 2012.
- 25 Kingslake, J., R. C. A. Hindmarsh, G. Aðalgeirsdóttir, H. Conway, H. F. J. Corr, F. Gillet-Chaulet, C. Martín, E. C. King, R. Mulvaney, and H. D. Pritchard: Full-depth englacial vertical ice sheet velocities measured using phase-sensitive radar, *J. Geophys. Res.: Earth Surface*, 119(12), 2604–2618, 2014.
- 30 Kjaer, H., Vallenga, P., Svensson, A., Elleskov, L., Kristensen, M., Tibuleac, C., Winstrup, M., and Kipfstuhl, S.: An optical dye method for continuous determination of acidity in ice cores, *Environ. Sci. Technol.*, es-2016-00026e, in review.

Formatted: Font: Italic

- Kjaer, H.: Continuous chemistry in ice cores—Phosphorus, pH and the photolysis of humic like substances, University of Copenhagen, PhD thesis, 2014.
- KNMI Climate Explorer, SAM time series <http://www.nerc-bas.ac.uk/iced/gima/sam.html>, WMO Regional Climate Centre, 2015a.
- 5 KNMI Climate Explorer, SOI time series <http://www.cru.uea.ac.uk/cru/data/soi.htm>, WMO Regional Climate Centre, 2015b.
- Kohno, M. and Fujii Y.: Past 220 year bipolar volcanic signals: remarks on common features of their source volcanic eruptions. *Ann. Glaciol.*, 35, 217–223, 2002.
- Krinner, G., Magand, O., Simmonds, I., Genthon, C., and Dufresne, J. L.: Simulated Antarctic precipitation and surface mass balance at the end of the 20th and 21st centuries, *Clim. Dynam.* 28, 215–230, doi:10.1007/s00382-006-0177-x, 2007.
- 10 Langway, C.C., Osada, Jr K., Clausen, H. B., Hammer, C.U., Shoji, H. and Mitani, A.: New chemical stratigraphy over the last millennium for Byrd Station, Antarctica. *Tellus*, 46B(1), 40–51, 1994.
- Lenaerts, J. T. M., van den Broeke, M. R., van den Berg, W. J., van Meijgaard, E., and Munneke, P. K.: A new, high resolution surface mass balance map of Antarctica (1979–2010) based on regional climate modeling, *Geophys. Res. Lett.*, 39, L04501, doi:10.1029/2011GL050713, 2012.
- 15 Lenaerts, J. T. M., van Meijgaard, E., van den Broeke, M. R., Ligtenberg, S. R. M., Horwath, M., and Isaksson, E.: Recent snowfall anomalies in Dronning Maud Land, East Antarctica, in a historical and future climate perspective, *Geophys. Res. Lett.*, 40, 1–5, doi : 10.1002/grl.50559, ~~URL~~ <http://doi.wiley.com/10.1002/grl.50559>, 2013.
- 20 Lenaerts, J.T.M., Brownvan, J., den Broeke, M. R., Matsuoka, K., Drews, R., Callens, D., Philippe, M., Gorodetskaya, I., van Meijgaard, E., Reymer, C., Pattyn, F., and van Lipzig, N. P.: High variability of climate and surface mass balance induced by Antarctic ice rises, *J. Glaciol.*, 60(224): 1101, 2014.
- Lenaerts, J. T. M., Vizcaino, M., Fyke, J., van Kampenhout, L., and van den Broeke, M. R.: Present-day and future Antarctic ice sheet climate and surface mass balance in the Community Earth System Model, *Clim. Dynam.*, online first, doi: 10.1007/s00382-015-2907-4, 2016 in press.
- 25 Levasseur, M.: Impact of Arctic meltdown on the microbial cycling of sulphur, *Nat. Geosci.*, 6, 691–700, 2013.
- Ludescher, J., Bunde, A., Franzke, C. L., and Schellnhuber, H. J.: Long-term persistence enhances uncertainty about anthropogenic warming of Antarctica, *Clim. Dyn.*, 1–9, 2015.
- 30

Field Code Changed

Field Code Changed

Formatted: English (United Kingdom)

Formatted: Font: Not Italic

Formatted: Indent: Left: 0", First line: 0"

Formatted: Indent: Left: 0", Hanging: 0.5"



Liboutry, L. A.: A critical review of analytical approximate solutions for steady-state velocities and temperature in cold ice sheets, *Zeitschrift für Gletscherkunde und Glazialgeologie* Bd., 15, 135–148, 1979.

Formatted: Indent: Left: 0", Hanging: 0.5"

Magand, O., Frezzotti, M., Pourchet, M., Stenni, B., Genoni, L., and Fily, M.: Climate variability along latitudinal and longitudinal transects in east Antarctica, *Ann. Glaciol.*, 39, 351–358, doi:10.3189/172756404781813961, 2004.

Magand, O., Genthon, C., Fily, M., Krinner, G., Picard, G., Frezzotti, M., and Ekaykin, A. A.: An up-to-date quality-controlled surface mass balance data set for the 90–180E Antarctica sector and 1950–2005 period, *J. Geophys. Res.*, 112, D12106, doi:10.1029/2006JD007691, 2007.

Marshall, G. J.: Trends in the southern annular mode from observations and reanalyses, *J. Climate*, 16, 4134–4143, 2003.

Matsuoka, K., Hindmarsh, R. C., Moholdt, G., Bentley, M. J., Pritchard, H. D., Brown, J., Conway, H., Drews, R., Durand, G., Goldberg, D., Hattermann, T., Kingslake, J., Lenearts, J., Martin, C., Mulvaney, R., Nicholls, K., Pattyn, F., Ross, N., Scambos, T., and Whitehouse, P.: –& Hattermann, T.: Antarctic ice rises and rumpled: their properties and significance for ice-sheet dynamics and evolution. *Earth-Sci. Rev.*, 150, 724–745, 2015.

Medley, B., Joughin, I., Das, S. B., Steig, E. J., Conway, H., Gogineni, S., Criscitiello, A. S., McConnell, J. R., Smith, B. E., van den Broeke, M. R., Lenaerts, J. T. M., Bromwich, D. H., and Nicolas, J. P.: Airborne-radar and ice-core observations of annual snow accumulation over Thwaites Glacier, West Antarctica confirm the spatiotemporal variability of global and regional atmospheric models, *Geophys. Res. Lett.*, 40(14), 3649–3654, 2013.

Formatted: Pattern: Clear

Monaghan, A. J., Bromwich, D. H., Fogt, R. L., Wang, S., Mayewski, P. A., Dixon, D. A., Ekaykin, A., Frezzotti, M., Goodwin, I., Isaksson, E., Kaspari, S. D., Morgan, V. I., Oerter, H., Van Ommen, T. D., van der Veen, C. J., and Wen, J.: Insignificant change in Antarctic snowfall since the International Geophysical Year, *Science*, 313, 827–831, doi:10.1126/science.1128243, 2006.

Formatted: Indent: Left: 0", Hanging: 0.5"

Moore, J. C., Narita, H., and Maeno, N.: A continuous 770-year record of volcanic activity from East Antarctica, *J. Geophys. Res.*, 96, 17353–17359, 1991.

Morgan, V. I., Goodwin, I. D., Etheridge, D. M., and Wookey, C. W.: Evidence for increased accumulation in Antarctica, *Nature*, 354, 58–60, 1991.

Mosley-Thompson, E., Paskievitch, J. F., Gow, A. J., and Thompson, L. G.: Late 20th century increase in South Pole snow accumulation, *J. Geophys. Res.*, 104, 3877–3886, 1999.

- Mulvaney, R., Pasteur, E.C. and Peel, D.A.: The ratio of MSA to non sea-salt sulphate in Antarctic peninsula ice cores, *Tellus*, 44b, 293-303, 1992.
- Mulvaney, R., Oerter, H., Peel, D. A., Graf, W., Arrowsmith, C., Pasteur, E. C., Knight, B., Littot, G. C., and Miners, W. D: 1000-year ice core records from Berkner Island, Antarctic, *Ann. Glaciol.*, 35, 45–51, doi:10.3189/172756402781817176, 2002.
- 5 Nishio, F., Furukawa, T., Hashida, G., Igarashi, M., Kameda, T., Kohno, M., Motoyama, H., Naoki, K., Satow, K., Suzuki, K., Morimasa, T., Toyama, Y., Yamada, T., and Watanabe, O.: Annual-layer determinations and 167 year records of past climate of H72 ice core in east Dronning Maud Land, Antarctica, *Ann. Glaciol.*, 35, 471–479, 2002.
- 10 ~~Nye, J.F.: Correction factor for accumulation measured by the thickness of the annual layers in an ice sheet. *J. Glaciol.*, 4(36), 785–788, 1963.~~
- Oerter, H., Graf, W., Wilhelms, F., Minikin, A., and Miller, H.: Accumulation studies on Amundsenisen, Dronning Maud Land, by means of tritium, DEP and stable isotope measurements: first results from the 1995/96 and 1996/97 field seasons, *Ann. Glaciol.*, 29, 1–9, doi:10.3189/172756499781820914, 1999.
- 15 Oerter, H., Wilhelms, F., Jung-Rothenhauser, F., Goktas, F., Miller, H., Graf, W., and Sommer, S.: Accumulation rates in Dronning Maud Land as revealed by DEP measurements at shallow firn cores, *Ann. Glaciol.*, 30, 27–34, 2000.
- ~~Palmer, C., Genthon, C., Claud, C., Kay, J. E., Wood, N. B. and L'Ecuyer, T.: Evaluation of current and projected Antarctic precipitation in CMIP5 models, *Clim.Dyn.*, online first, doi:10.1007/s00382-016-3071-1, 2016.~~
- 20 ~~Parrenin, F., Dreyfus, G., Durand, G., Fujita, S., Gagliardini, O., Gillet, F., Jouzel, J., Kawamura, K., Lhomme, N., Masson-Delmotte, V., Ritz, C., Schwander, J., Shoji, H., Uemura, R., Watanabe, O., and Yoshida, N.: 1-D-ice flow modelling at EPICA Dome C and Dome Fuji, East Antarctica, *Clim. Past*, 3, 243–259, doi:10.5194/cp-3-243-2007, 2007.~~
- ~~Parrenin, F., Dreyfus, G., Durand, G., Fujita, S., Gagliardini, O., Gillet, F., ... & Yoshida, N.: 1-D-ice flow modelling at EPICA Dome C and Dome Fuji, East Antarctica. *Clim. Past*, 3(2), 243–259, 2007.~~
- 25 ~~Polvani, L. M., Waugh, D. W., Correa, G. J., & Son, S. W.: Stratospheric ozone depletion: The main driver of twentieth-century atmospheric circulation changes in the Southern Hemisphere. *J. Climate*, 24(3), 795–812, 2011.~~
- 30 Raymond, C., Weertman, B., Thompson, L., Mosley-Thompson, E., Peel, D., and Mulvaney, R.: Geometry, motion and balance of Dyer Plateau, Antarctica, *J. Glaciol.*, 42, 510–518, 1996.

Formatted: English (United Kingdom)

- Ren, J., Li, C., Hou, S., Xiao, C., Qin, D., Li, Y., and Ding, M.: A 2680 year volcanic record from the DT-401 East Antarctic ice core, *J. Geophys. Res.*, 115, D11301, doi:10.1029/2009JD012892, 2010.
- Rignot, E., Velicogna, I., van den Broeke, M. R., Monaghan, A., and Lenaerts, J.: Acceleration of the contribution of the Greenland and Antarctic ice sheets to sea level rise, *Geophys. Res. Lett.*, 38, L05503, doi:10.1029/2011GL046583, 2011.
- Roberts, J., Plummer, C., Vance, T., van Ommen, T., Moy, A., Poynter, S., Treverrow, A., Curran, M., and George, S.: A 2000-year annual record of snow accumulation rates for Law Dome, East Antarctica, *Clim. Past*, 11, 697–707, doi:10.5194/cp-11-697-2015, 2015.
- Roberts, J., Plummer, C., Vance, T., van Ommen, T., Moy, A., Poynter, S., ... & George, S.: A 2000-year annual record of snow accumulation rates for Law Dome, East Antarctica, *Clim. Past*, 11(5), 697–707, 2015.
- Rupper, S., Christensen, W. F., Bickmore, B. R., Burgener, L., Koenig, L. S., Koutnik, M. R., ~~...~~ Miège, C., & Forster, R. R.: The effects of dating uncertainties on net accumulation estimates from firn cores. *J. Glaciol.*, 61(225), 163–172, 2015.
- Ruth, U., Wagenbach, D., Mulvaney, R., Oerter, H., Graf, W., Pulz, H., and Littot, G.: Comprehensive 1000 year climate history from an intermediate depth ice core from the south dome of Berkner Island, Antarctica: methods, dating and first results, *Ann. Glaciol.*, 39, 146–154, 2004.
- Savitzky A., and Golay, M. J. E.: Smoothing and Differentiation of Data by Simplified Least Squares Procedures. *Anal. Chem.*, 36 (8), pp 1627–1639, DOI: 10.1021/ac60214a047, 1964.
- Schlosser, E., and Oerter, H.: Shallow firn cores from Neumayer, Ekströmis, Antarctica: a comparison of accumulation rates and stable-isotope ratios, *Ann. Glaciol.*, 35, 91–96, 2002.
- Schlosser, E., Manning, K. W., Powers, J. G., Duda, M. G., Birnbaum, G., and Fujita, K.: Characteristics of high-precipitation events in Dronning Maud Land, Antarctica, *J. Geophys. Res.*, 115, D14107, doi:10.1029/2009JD013410, 2010.
- Schlosser, E., Anshütz, H., Divine, D., Martma, T., Sinisalo, A., Altnau, S., and Isaksson, E.: Recent climate tendencies on an East Antarctic ice shelf inferred from a shallow firn core network, *J. Geophys. Res.*, 119, 6549–6562, 2014.
- Shepherd, A., Ivins, E. R., Geruo, A., Barletta, V. R., Bentley, M. J., Bettadpur, S., Briggs, K. H., Bromwich, D. H., Forsberg, R., Galin, N., Horwath, M., Jacobs, S., Joughin, I., King, M. A., Lenaerts, J. T. M., Li, J., Lichtenberg, S. R. M., Luckman, A., Luthcke, S. B., McMillan, M., Meister, R., Milne, G., Mouginot, J., Muir, A., Nicolas, J. P., Paden, J., Payne, A. J., Pritchard, H., Rignot, E., Rott, H., Sørensen, L. S., Scambos, T. A., Scheuchl, B., Schrama, E. J. O., Smith, B., Sundal, A. V., van Angelen, J. H., van de

Formatted: English (United States)

Formatted: Not Highlight

[Berg, W. J., van den Broeke, M. R., Vaughan, D. G., Velicogna, I., Wahr, J., Whitehouse, P. L., Wingham, D. J., Yi, D., Young, D., and Zwally, H. J. & Horwath, M.: A reconciled estimate of ice-sheet mass balance, Science, 338\(6111\), 1183–1189, 2012.](#)

[Sommer, S., Appenzeller, C., Röthlisberger, R., Hutterli, M. A., Stauffer, B., Wagenbach, D., Oerter, H., Wilhelms, F., Miller, H., and Mulvaney, R.: Glacio-chemical study spanning the past 2 kyr on three ice cores from Dronning Maud Land, Antarctica, 1. Annually resolved accumulation rates, J. Geophys. Res., 105, 29411–29421, 2000.](#)

[Sigl, M., McConnell, J. R., Layman, L., Maselli, O., McGwire, K., Pasteris, D., ... & Mulvaney, R.: A new bipolar ice core record of volcanism from WAIS Divide and NEEM and implications for climate forcing of the last 2000 years. Journal of Geophysical Research: Atmospheres, 118\(3\), 1151–1169, 2013.](#)

[Steig, E., Fischer, H., Fisher, D., Frezzotti, M., Mulvaney, R., Taylor, K., Wolff, E.: The IPICS 2k Array: a network of ice core climate and climate forcing records for the last two millennia, <http://www.pages-igbp.org/ipics/> IPICS \(International Partnership in Ice Core Science\), 2005.](#)

[Stenni, B., Caprioli, R., Cimmino, L., Cremisini, C., Flora, O., Gragnani, R., Longinelli, A., Maggi, V., and Torcini, S.: 200 years of isotope and chemical records in a firm core from Hercules Neve, northern Victoria Land, Antarctica, Ann. Glaciol., 29, 106–112, 1999.](#)

[Stenni, B., Proposito, M., Gragnani, R., Flora, O., Jouzel, J., Falourd, S., and Frezzotti, M.: Eight centuries of volcanic signal and climate change at Talos Dome \(East Antarctica\), J. Geophys. Res., 107, 4076, doi:10.1029/2000JD000317, 2002.](#)

[Sommer, S., Appenzeller, C., Röthlisberger, R., Hutterli, M. A., Stauffer, B., Wagenbach, D., Oerter, H., Wilhelms, F., Miller, H., and Mulvaney, R.: Glacio-chemical study spanning the past 2 kyr on three ice cores from Dronning Maud Land, Antarctica, 1. Annually resolved accumulation rates, J. Geophys. Res., 105, 29411–29421, 2000.](#)

[Takahashi, H., Yokoyama, T., Igarashi, M., Motoyama, H., and Suzuki, K.: Resolution of environmental variation by detail analysis of YM85 shallow ice core in Antarctica, Bull. Glaciol. Res., 27, 16–23, 2009.](#)

[Thomas, E. R., Marshall, G. J., and McConnell, J. R.: A doubling in snow accumulation in the western Antarctic Peninsula since 1850, Geophys. Res. Lett., 35, L01706, doi:10.1029/2007GL032529, 2008.](#)

[Thomas, E. R., Hosking, J. S., Tuckwell, R. R., Warren, R.A., and Ludlow, E.C.: Twentieth century increase in snowfall in coastal West Antarctica, Geophys. Res. Lett., 42, 9387–9393, doi:10.1002/2015GL065750, 2015.](#)

Formatted: Indent: Left: 0", Hanging: 0.5"

- Traufetter, F., Oerter, H., Fischer, H., Weller, R., ~~&and~~ Miller, H.: Spatio-temporal variability in volcanic sulphate deposition over the past 2 kyr in snow pits and firn cores from Amundsenisen, Antarctica., ~~J.ournal of Glaciol.egy~~, 50(168), 137–146, 2004.
- 5 ~~Turner, J., Colwell, S. R., Marshall, G. J., Lachlan-Cope, T. A., Carleton, A. M., Jones, P. D., Lagun, V., Reid, P. A. and Iagovkina, S.: Antarctic climate change during the last 50 years, Int. J. Climatol., 25: 279–294, doi:10.1002/joc.1130, 2005.~~
- 15 van de Berg, W. J., van den Broeke, M. R., Reijmer, C. H., and van Meijgaard, E.: Reassessment of the Antarctic SMB using calibrated output of a regional atmospheric climate model, J. Geophys. Res., 111, D11104, doi:10.1029/2005JD006495, -2006.
- van den Broeke, M., van de Berg, W. J., and van Meijgaard, E.: Snowfall in coastal West Antarctica much greater than previously assumed, Geophys. Res. Lett., 33, L02505, doi:10.1029/2005GL025239, 2006.
- van Ommen, T. D., and Morgan, V.: Snowfall increase in coastal East Antarctica linked with southwest Western Australian drought, Nat. Geosci., 3, 267–272, doi:10.1038/ngeo761, 2010.
- 20 Vaughan, D.G., Comiso, J.C., Allison, I., Carrasco, J., Kaser, G., Kwok, R., Mote, P., Murray, T., Paul, F., Ren, J., Rignot, E., Solomina, O., Steffen, K., and Zhang, T.: Observations: Cryosphere. In: Climate Change 2013: The Physical Science Basis. Contribution of Working Group I to the Fifth Assessment Report of the Intergovernmental Panel on Climate Change [Stocker, T.F., D. Qin, G.-K. Plattner, M. Tignor, S.K. Allen, J. Boschung, A. Nauels, Y. Xia, V. Bex and P.M. Midgley (eds.)]. Cambridge University Press, Cambridge, United Kingdom and New York, NY, USA, 2013.
- 25 ~~Wang, Y., Ding, M., van Wessem, J., Schlosser, E., Altnau, S., van den Broeke, M., Lenaerts, J., Thomas, E., Isaksson, E., Wang, J., and Sun, W.: A comparison of Antarctic Ice Sheet surface mass balance from atmospheric climate models and in situ observations, J. Climate, doi:10.1175/JCLI-D-15-0642.1, early online release, 2016.~~
- 30 Wolff, E. W., Jones, A. E., Bauguitte, S. B., ~~&and~~ Salmon, R. A.: The interpretation of spikes and trends in concentration of nitrate in polar ice cores, based on evidence from snow and atmospheric measurements, ~~-Atmos. Chem. Phys. Atmospheric Chemistry and Physics~~, 8(18), 5627–5634, 2008.
- Xiao, C., Mayewski, P. A., Qin, D., Li, Z., Zhang, M., and Yan, Y.: Sea level pressure variability over the southern Indian Ocean inferred from a glaciochemical record in Princess Elizabeth Land, east Antarctica, J. Geophys. Res., 109, D16101, doi:10.1029/2003JD004065, 2004.
- 35

Formatted: Indent: Left: 0", Hanging: 0.5"

Formatted: Font: (Default) Times New Roman, 10 pt, Font color: Auto, Pattern: Clear

Formatted: Font: (Default) Times New Roman, 10 pt, Font color: Auto, Pattern: Clear

Formatted: Font: (Default) Times New Roman, 10 pt, Font color: Auto, Pattern: Clear

Formatted: French (Belgium)

Formatted: French (Belgium)

Formatted: French (Belgium)

Zhang, M. J., Li, Z. Q., Xiao, C. D., Qin, D. H., Yang, H. A., Kang, J. C., & Li, J.: A continuous 250-year record of volcanic activity from Princess Elizabeth Land, East Antarctica. *Antarctic Science*, 14(01), 55–60, 2002.

5 Zhang, M., Li, Z., Ren, J., Xiao, C., Qin, D., Kang, J., and Li, J.: 250 years of accumulation, oxygen isotope and chemical records in a firm core from Princess Elizabeth Land, East Antarctica, *J. Geogr. Sci.*, 16, 23–33, doi:10.1007/s11442-006-0103-5, 2006.

## Tables

Table 1. Characteristics of the 12 volcanic peaks found in the IC12 core, and used to constrain the depth-age relationship to an uncertainty of  $\pm 2$  year. Bold years were used as reference for average accumulation calculations by period in Figure 6. Ref.: references: 1) Traufetter et al., 2004 and references therein ; 2) Kaczmariska et al., 2004 ; 3) Nishio et al., 2002 ; 4) Stenni et al., 2002 ; 5) Kohno and Fuji, 2002 ; 6) Zhang et al., 2002 ; 7) Moore et al., 1991 ; 8) Langway et al., 1994. \*identified from ion chromatography.

Probable source volcano	Year of eruption	Year of deposition	VEI	Depth (m)	Difference between assigned age and year of deposition	Ref.
Unknown		2009		4.822		
Unknown		1995		20.01		
Pinatubo	1991	<b>1992 <math>\pm 1</math></b>	6	23.095	0	1
El Chichon	1982	<b>1982 <math>\pm 1</math></b>	4	33.63	-2	1
Unknown		1976		36.42		
Unknown		1973		38.58		
Unknown		1966		44.08		
Agung	1963	<b>1964 <math>\pm 1</math></b>	4	45.95	-1	1
Unknown		1961		47.15		
Carran-Los Venados	1955	<b>1955 <math>\pm 1</math></b>	4	50.79	0	2, 3
Unknown		1945		56.37		
Unknown		1940		59.24		
Unknown		1936		61.445		
Cerro Azul	1932	<b>1932 <math>\pm 1</math></b>	5	62.92	0	1
Unknown		1930		63.81		
Unknown		1922		67.26		
Unknown		1918		69.05		
Unknown		1916		69.82		
Unknown		1912		71.745		
Unknown		1908		73.49		
Santa Maria	1902	<b>1902 <math>\pm 1</math></b>	5	75.03	1	2, 4, 5
Unknown		1892		78.84		
Krakatau	1883	<b>1884 <math>\pm 1</math></b>	6	82.237*	0	1
Unknown		1844		94.98		
Coseguina	1835	<b>1835 <math>\pm 1</math></b>	5	97.34	0	1
Galunggung	1822	<b>1822 <math>\pm 1</math></b>	5	101.3	-1	2, 5, 6
Tambora	1815	<b>1816 <math>\pm 1</math></b>	7	102.4	2	1
Unknown	1809 $\pm 2$	<b>1809 <math>\pm 3</math></b>	?	104	2	1
Cotopaxi	1768	<b>1768 <math>\pm 1</math></b>	4	115.3	-1	2, 7, 8
Planchon-Peteroa	1762	<b>1762 <math>\pm 1</math></b>	4	116.2	1	1
Unknown		1759		117.4		
Unknown		1750		119.2		
Unknown		1747		119.9		

Table 1. Mean accumulation rates at IC12 for different time periods

<u>Period (years A.D.)</u>	<u>Accumulation (m w.e. a<sup>-1</sup>) (oldest estimate)</u>	<u>Accumulation (m w.e. a<sup>-1</sup>) (youngest estimate)</u>	<u>Mean accumulation (m w.e. a<sup>-1</sup>)</u>
<u>1816–2011</u>	<u>0.476</u>	<u>0.513</u>	<u>0.495</u>
<u>1816–1961</u>	<u>0.432</u>	<u>0.476</u>	<u>0.454</u>
<u>1962–2011</u>	<u>0.604</u>	<u>0.623</u>	<u>0.614</u>
<u>1816–1991</u>	<u>0.459</u>	<u>0.498</u>	<u>0.479</u>
<u>1992–2011</u>	<u>0.626</u>	<u>0.651</u>	<u>0.638</u>

Table 2. Accumulation rates of the last 10 years from IC12 ice core (oldest and youngest estimates, see text for details)

<u>Year (A.D.)</u>	<u>Accumulation (m w.e. a<sup>-1</sup>) (oldest estimate)</u>	<u>Accumulation (m w.e. a<sup>-1</sup>) (youngest estimate)</u>
<u>2011</u>	<u>0.980</u>	<u>0.980</u>
<u>2010</u>	<u>0.641</u>	<u>0.641</u>
<u>2009</u>	<u>0.824</u>	<u>0.824</u>
<u>2008</u>	<u>0.651</u>	<u>0.651</u>
<u>2007</u>	<u>0.287</u>	<u>0.699</u>
<u>2006</u>	<u>0.419</u>	<u>0.661</u>
<u>2005</u>	<u>0.661</u>	<u>0.681</u>
<u>2004</u>	<u>0.681</u>	<u>0.666</u>
<u>2003</u>	<u>0.666</u>	<u>0.621</u>
<u>2002</u>	<u>0.621</u>	<u>0.891</u>

Table 2. Average accumulation rates at IC12 for various time periods framed by volcanic horizons. The first year of each period is included, not the second (ex: 1768–2012: includes 1768, not 2012). Nye: correction for a linear decrease of annual layer thickness with depth. D-J: Corrected using a strain rate of 0.003 a<sup>-1</sup> which is the slope of the annual layer thickness (in m w.e.) vs. depth relationship before 1900.

Table 3. Accumulation for the last 10 years from IC12 ice core. \*See Table 2 legend and text for explanation  
\*\*not a full year

Formatted: Left, Line spacing: single, Pattern: Clear



Figure S1. Full vertical profile of water stable isotopes with a grey and black band on the left indicating sections of 10-cm and 5-cm resolution, respectively (a); major ion (b-f), normalized ECM conductivity expressed as multiple of standard deviation ( $\sigma$ ) (light grey: 1-mm resolution, dark grey: 0.05 m-running mean). The  $4\sigma$  threshold is shown as a dotted vertical line, and identified volcanic peaks as dashed grey horizontal lines (g); annual layer

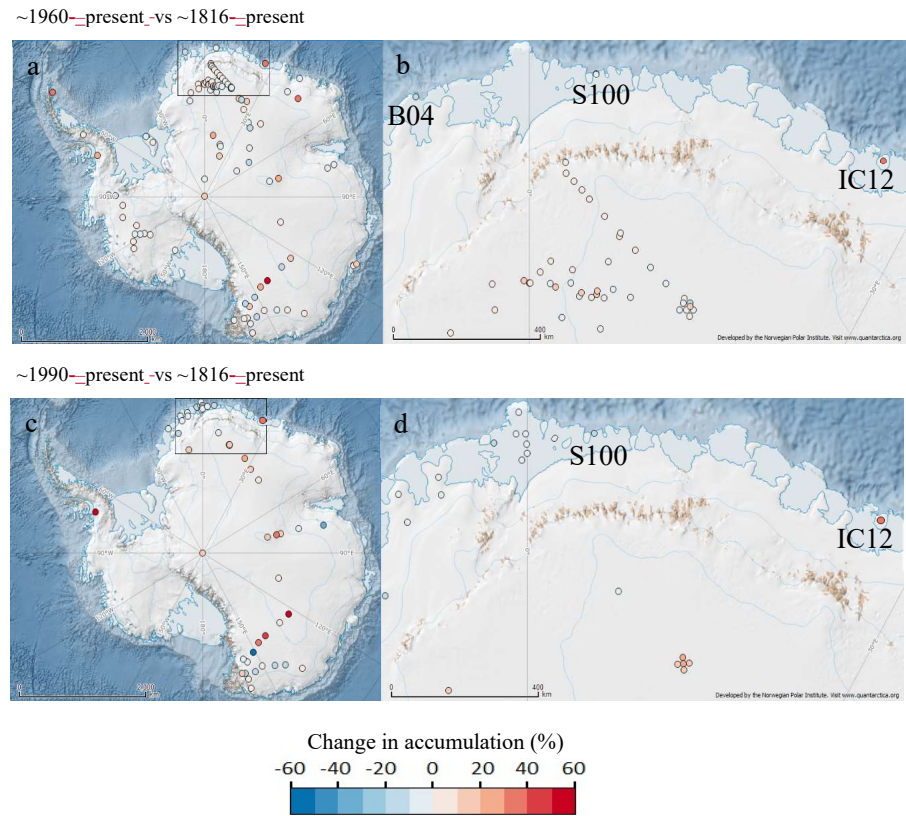


Figure S1. Full vertical profile of water stable isotopes with a grey and black band on the left indicating sections of 10-cm and 5-cm resolution, respectively (a); major ion (b-f), normalized ECM conductivity expressed as multiple of standard deviation ( $\sigma$ ) (light grey: 1-mm resolution, dark grey: 0.05 m-running mean). The  $4\sigma$  threshold is shown as a dotted vertical line, and identified volcanic peaks as dashed grey horizontal lines (g); annual layer

boundaries in the youngest (Green) and the oldest (Blue) estimates. Each colour transition indicates a boundary (h).

Figure S2. Full vertical profile, as in Fig. S1 but split in 17 sections for more visibility.

5

Figure 1: Location of IC12 and other ice cores referred to herein. Difference in mean annual SMB between the period ~1960–present and the period ~1816–present (see Table A1 for exact periods) (a-b). Same as (a-b) for the period ~1990–present compared to ~1816–present (c-d). Panels (b) and (d) are expansions of the framed areas in panels (a) and (c).

10

Figure 1: Location of IC12 and other ice cores referred to in the discussion. Difference in mean annual SMB for the periods ~1960–present (a-b), and ~1990–present (c-d), compared to the period ~1816–present (see Table A1 for exact periods). Panels (b) and (d) are zooms of the framed areas in panels (a) and (c).

Figure 1: Location of IC12 and other ice cores referred to in the discussion. Change in Accumulation between ~1960–present average compared to ~1816–present average (a-b) and ~1990–present compared to 1816–present (c-d), see Table A1 for exact periods. Panels (b) and (d) are zoomed of the framed zone in panels (a) and (c).

15

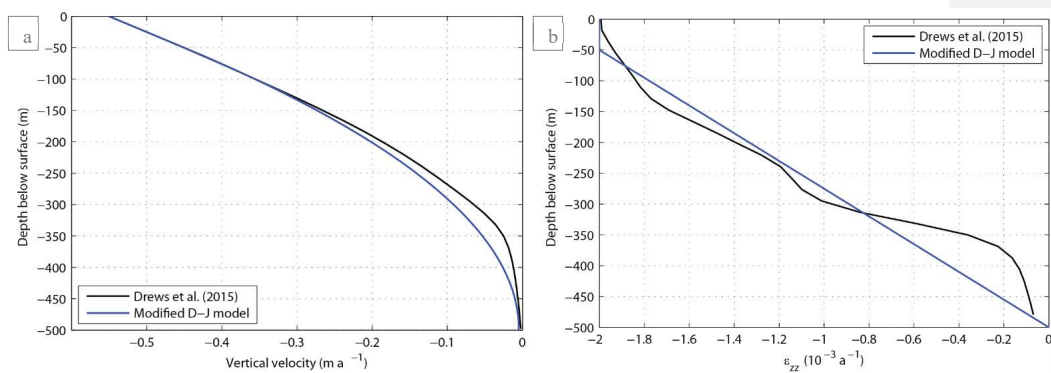


Fig. 2. Vertical velocity (a) and vertical strain rate (b) profiles, according to the modified Dansgaard-Johnsen model (blue) and the full Stokes model (black, Drews et al., 2015).

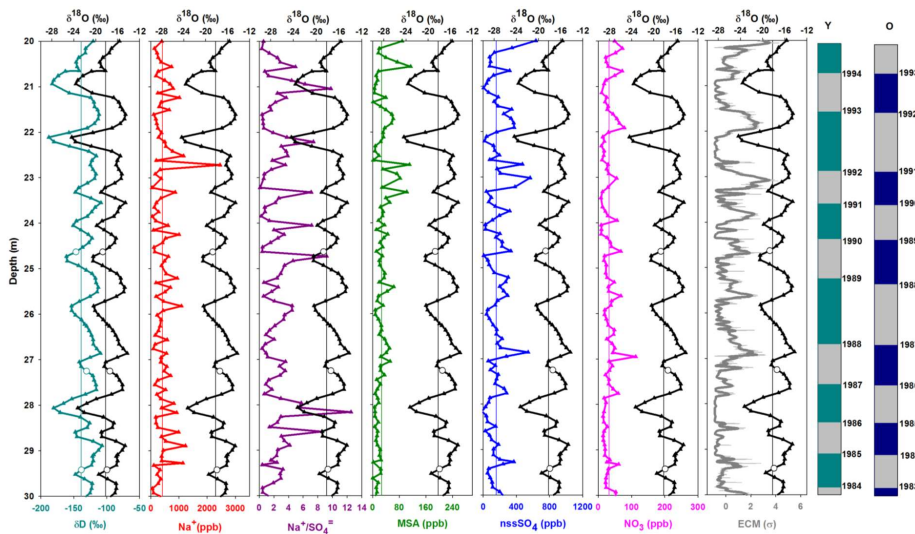


Fig. 3. A 10 m long illustrative example of how variations in stable isotopes ( $\delta^{18}\text{O}$ ,  $\delta\text{D}$ ), chemical species (and/or their ratios) and smoothed ECM (running mean, 0.1 m) are used to identify annual layers. Coloured bars on the right indicate the annual layer boundaries (middle depth of each period corresponding to above average  $\delta^{18}\text{O}$  values) for the youngest (Y) and oldest (O) estimates, with 1 year difference at 20 m depth. See Fig. S1 and S2 for the whole profile. White dots in the  $\delta^{18}\text{O}$  and  $\delta\text{D}$  profiles indicate thin ice layers identified visually in the core. Figure 2. Variations in stable isotopes ( $\delta^{18}\text{O}$ ,  $\delta\text{D}$ ), smoothed ECM (running mean, 0.1 m), chemical species and their ratios used to constrain annual layer thickness in an example 10 m long section (20–30 m depth) of the IC12 ice core. Dashed horizontal lines indicate the annual layer limit (middle of the summer  $\delta^{18}\text{O}$  peak).

10

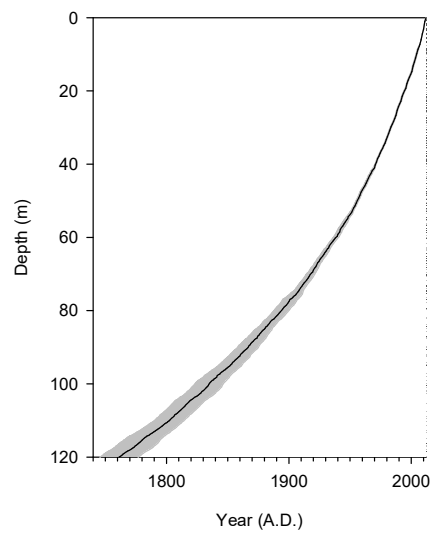


Fig. 4. Age-depth relationship for IC12 reconstructed from the relative dating process. Grey shading shows the uncertainty range between the oldest and the youngest estimates. At the bottom, the uncertainty is  $\pm 16$  years.

Figure 3. Age-depth relationships reconstructed from the relative dating process. Note that the approach results in no uncertainty above 62.38 m depth (year 1933). At 120 m depth, the uncertainty is  $\pm 10$  years.

Field Code Changed

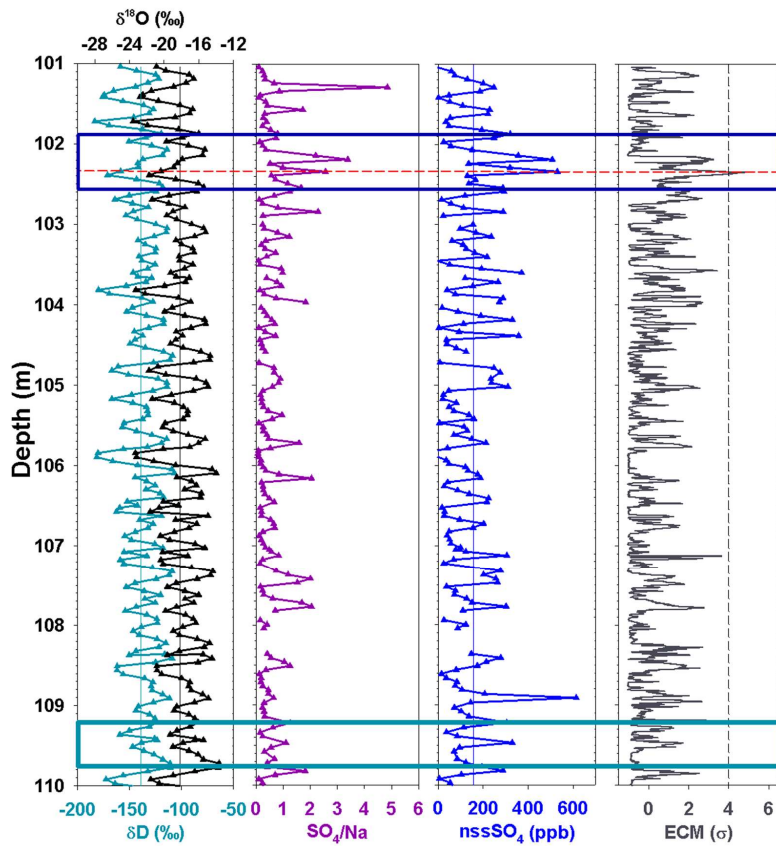


Fig. 5. Variations in stable isotopes ( $\delta^{18}\text{O}$ ,  $\delta\text{D}$ ) and volcanic indicators in the IC12 ice core section where the Tambora 1815 eruption is expected (101–110 m depth). Boxes indicate the expected depth of this eruption according to the youngest (light blue, bottom) and the oldest (dark blue, top) age–depth chronologies determined on the basis of our relative core dating. The dashed horizontal red line indicates the identified Tambora peak. The dashed vertical black line shows the ECM  $4\sigma$  threshold.

5

Figure 4. Continuous record of ECM (except for 6 measurement gaps shown as grey bands). Normalized conductivity (black line) is expressed as multiple of standard deviation ( $\sigma$ ). The  $2\sigma$  threshold is shown as a dotted vertical line, and identified volcanic peaks as dashed grey horizontal lines.

- 5 Figure 5. Annual layer thickness plotted against depth. The record is divided into two age/depth ranges, before and after 1900/49 m, for which best fit straight lines are presented. We use the hypothesis that no temporal drift in annual accumulation existed prior to 1900 (see text for details).

Field Code Changed

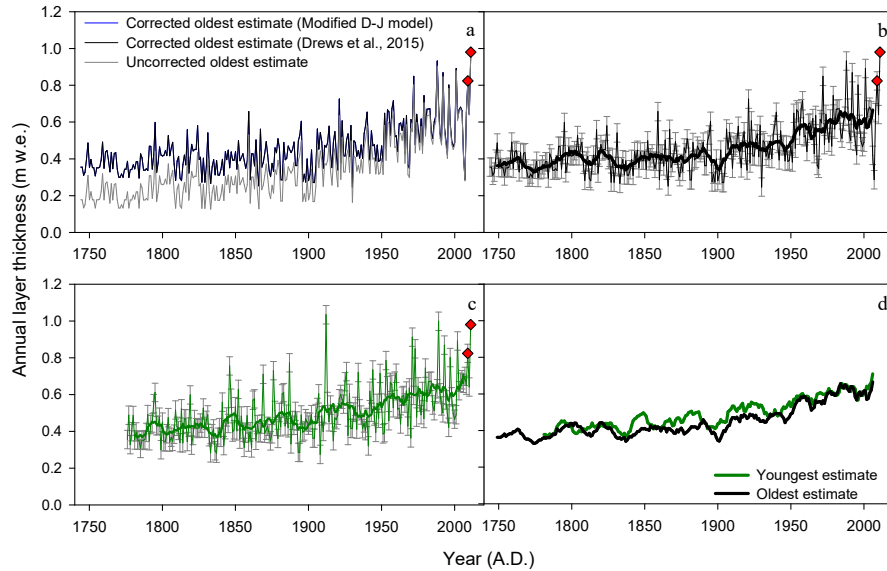


Fig. 6. Annual layer thicknesses at IC12 in m w.e.: for the oldest estimate: uncorrected annual layer thickness (grey line), corrected annual layer thickness using full Stokes Dews et al. (2015) model (black line) and corrected annual layer thickness with the modified Dansgaard-Johnsen model (blue line, undistinguishable from the black line at this scale) (a); corrected annual layer thickness using Dews et al. (2015) model with error bars (thin black line) and 11 year running mean (thick black line) for the oldest estimate (b) and the youngest estimate (green lines) (c). Comparison of youngest (green) and oldest (black) estimates with an 11 year running mean (d). Red diamonds highlight years 2009 and 2011, discussed in the text.

Figure 6. Accumulation rates at IC12. (a) Annual (thin lines with error bars) and average (11 years running mean, thick lines) accumulation rates. The blue lines show uncorrected annual layer thickness in m w.e. The red diamonds highlight years 2009 and 2011 discussed in the text (a-b) Corrected annual layer thicknesses are shown by green lines for the Nye approach and black lines for the Dansgaard and Johnsen approach (see text for details). (b) Dotted horizontal lines represent long-term accumulation (mean plus standard deviation and mean minus standard



deviation) for various time periods bounded by specific volcanic eruption events (indicated by vertical lines and bold years).

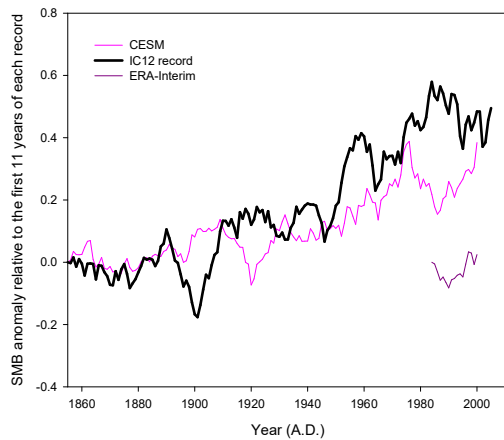


Fig. 7. Comparison between trends in IC12 record (oldest estimate, thick black line), CESM output (pink line) and ERA-Interim reanalysis (dark pink line) represented as relative anomaly of 11 year running mean with respect to the first 11 years of each record, for the overlapping period 1850–2011.

Field Code Changed

Formatted: Pattern: Clear

Figure 7. Large-scale atmospheric, ocean and sea-ice anomalies in (a) high-accumulation (10% highest) and (b) low-accumulation (10% lowest) years in the CESM historical time series (1850-2005). The colours show the annual mean near-surface temperature anomaly (in °C), the lines show the surface pressure anomaly (in hPa), and the stippled/hatched areas show the anomaly in sea-ice coverage (stippled areas are areas with >20 days less sea ice cover than the mean, hatched areas show areas with >20 days more sea ice than the mean). The green star shows the location of the ice core.

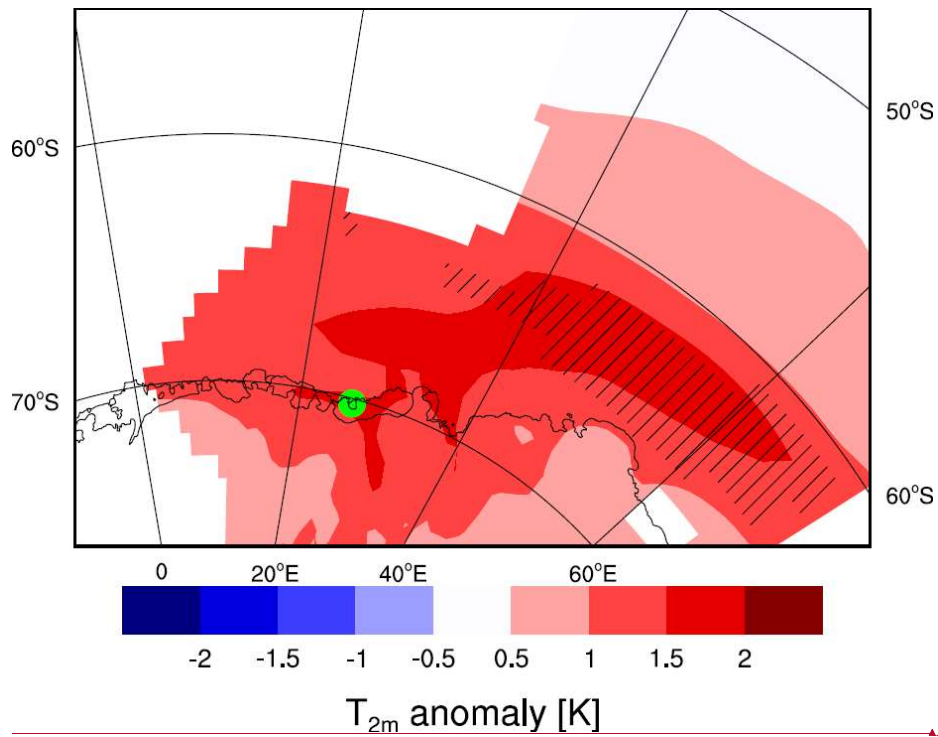


Fig. 8. Large-scale atmospheric, ocean and sea-ice anomalies in high-accumulation (10 % highest) years in the CESM historical time series (1850–2005). The colours show the annual mean near-surface temperature anomaly (in °C), and the hatched areas show the anomaly in sea-ice coverage (>20 days less sea ice cover than the mean).

5 The green dot shows the location of the ice core.

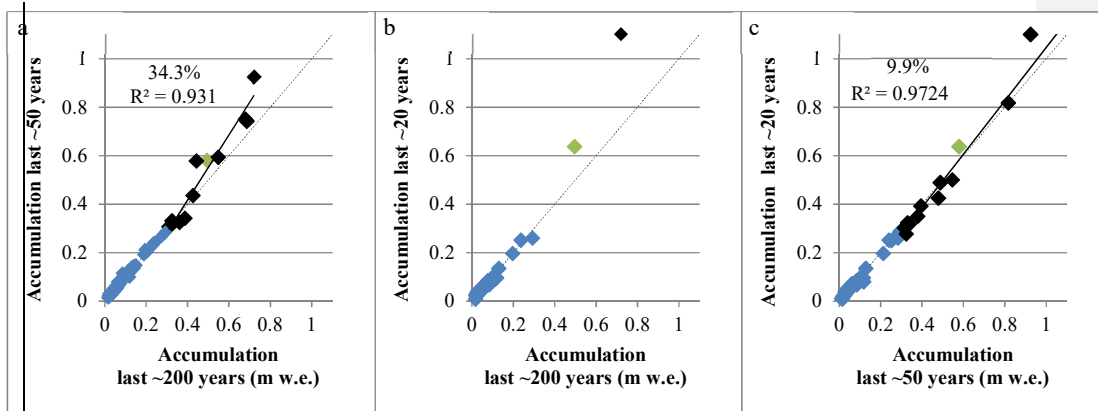


Fig. 9. Comparison of SMB between (a) the last ~200 years and the last ~50 years (a), (b) the last ~200 years and the last ~20 years (b), and (c) the last ~50 years and the last ~20 years (c). See Table A1 for exact periods. Sites above 0.3 m w.e.  $a^{-1}$  are shown in black, with the exception of our study site, IC12, which is shown in green. Sites below 0.3 m w.e.  $a^{-1}$  are shown in blue. The black lines show a linear regression through high accumulation sites. Increases in % between the periods compared are shown on the graph with  $R^2$  value when relevant. The 1:1 slope (0 % change) is shown as a dotted line.

## Appendix A

Table A1. Sites information and snow accumulation values \*no significant trend during the 20<sup>th</sup> century \*\*short record: only recent periods are compared \*\*\*when only a stacked accumulation change is given, accumulation from individual ice cores are inferred from the stacked record as if it was the same trend for all ice cores. Ref : reference period. Numbers in *italic* are inferred from the trend given in the referenced paper

Site name	Latitude	Longitude	Elevation (m a.s.l.)	Last ~200 years (10 <sup>-3</sup> m w.e.) (kg m <sup>-2</sup> a <sup>-1</sup> )	Accumulation (10 <sup>-3</sup> m w.e.) (kg m <sup>-2</sup> a <sup>-1</sup> )	Last ~50 years	Accumulation (10 <sup>-3</sup> m w.e.) (kg m <sup>-2</sup> a <sup>-1</sup> )	Last ~20 years	Accumulation (10 <sup>-3</sup> m w.e.) (kg m <sup>-2</sup> a <sup>-1</sup> )	% change (50a - ref)	% change (20a - ref) except**	Method	Study
Siple Dome	-81.6530	-148.9980	620	1890–1994	120	1922–1991	118			-2 %		Ice core	Kaspari et al., 2004
ITASE00-5	-77.6830	-123.9950	1828	1716–2000	140	1922–1991	141			1 %		Ice core	Kaspari et al., 2004
ITAE99-1	-80.6200	-122.6300	1350	1724–1998	139	1922–1991	146			5 %		Ice core	Kaspari et al., 2004
ITASE00-4	-78.0830	-120.0800	1697	1799–2000	189	1922–1991	193			2 %		Ice core	Kaspari et al., 2004
RIDS C	-80.0100	-119.4300	1530	1903–1995	112	<i>1970–1995</i>	<i>108.35</i>			-3 %		Ice core	Kaspari et al., 2004
RIDS B	-79.4600	-118.0500	1603	1922–1995	150	<i>1970–1995</i>	<i>149.37</i>			0 %		Ice core	Kaspari et al., 2004
RIDS A	-78.7300	-116.3300	1740	1831–1995	235	1922–1991	234			0 %		Ice core	Kaspari et al., 2004
ITASE00-1	-79.3830	-111.2390	1791	1653–2001	220	1922–1991	222			1 %		Ice core	Kaspari et al., 2004
ITASE01-2	-77.8430	-102.9100	1353	1890–2001	427	1922–1991	436			2 %		Ice core	Kaspari et al., 2004
ITASE01-3	-78.1200	-95.6460	1633	1859–2001	325	1922–1991	331			2 %		Ice core	Kaspari et al., 2004
ITASE01-5	-77.0590	-89.1370	1246	1780–2001	388	1922–1991	342			-12 %		Ice core	Kaspari et al., 2004
ITASE01-6	-76.0970	-89.0170	1232	**		1978–1990	395	<i>1978–1999</i>	<i>392.6</i>	-1 %		Ice core	Kaspari et al., 2004
Gomez	-73.5900	-70.3600	1400	1855–2006	720	1970s–2006	925	1997–2006	1100	28 %	53 %	Ice core	Thomas et al., 2008
Dyer Plateau	-70.6700	-64.8900	2002	1790–1989	549	1969–1989	593			8 %		Ice core	Raymond et al., 1996
James Ross Island	-64.2200	-57.6800	1640	1847–1980	443	1964–1990	578			30 %		Ice core	Aristarain et al., 2004
R1	-78.3075	-46.2728	718	1816–1998	204	*	<i>204</i>			0 %		Ice core	Mulvaney et al., 2002
Berkner B25	-79.5700	-45.7200	890	1816–1956	131	1965–1994	141			8 %		Ice core	Ruth et al., 2004
A	-72.6500	-16.6333	60	**		1975–1989	380	1980–1989	350	-8 %		Ice core	Isaksson and Melvold, 2002
E	-73.6000	-12.4333	700	**		1932–1991	324	1980–1991	277	-15 %		Ice core	Isaksson and Melvold, 2002;
													Isaksson et al., 1996
B39	-71.4100	-9.9000	655	**		1935–2007	818	<i>1987–2007</i>	<i>818</i>		0 %	Ice core	Fernandoy et al., 2010
FB0704	-72.0600	-9.5600	760	**		1962–2007	489	<i>1987–2007</i>	<i>489</i>		0 %	Ice core	Fernandoy et al., 2010
BAS-depot	-77.0333	-9.5000	2176	1816–1997	71	1965–1997	71			0 %		Ice core	Hofstede et al., 2004
B04	-70.6200	-8.3700	35	1892–1981	362	±95 1960–1980	325			-10 %			Schlosser and Oerter, 2002
CV	-76.0000	-8.0500	2400	1816–1997	62	1965–1997	68	±2 1992–1997	70	10 %	13 %	Ice core	Karlof et al., 2005
B38	-71.1600	-6.7000	690	**		1960–2007	1257	<i>1987–2007</i>	<i>1257</i>		0 %	Ice core	Fernandoy et al., 2010
FB0702	-71.5700	-6.6700	539	**		1959–2007	547	<i>1987–2007</i>	<i>500</i>		-9 %	Ice core	Fernandoy et al., 2010
FB9816	-75.0000	-3.5037	2740	1800–1997	47	±17 1950–1997	<i>51.5****</i>			10 %		Ice core	Oerter et al., 2000
B31	-75.5800	-3.4300	2669	1816–1997	58.4	1966–1989	59.8			2 %		Ice core	Oerter et al., 2000
H	-70.5000	-2.4500	53	**		1953–1993	480	1980–1993	425	-11 %		Ice core	Isaksson and Melvold, 2002
NUS08-2	-87.8500	-1.8000	2583	1815–2007/8	67.4	±2.6 1963–2007/8	63.4	±4.2		-6 %		Ice core	Anschutz et al., 2011
S32	-70.3100	-0.8000	53	**		1995–2009	339	±36		-6 %		Ice core	Schlosser et al., 2014
G3	-69.8230	-0.6120	57	**		1993–2009	295	±29		-2 %		Ice core	Schlosser et al., 2014
FB9815	-74.9492	-0.5055	2840	1801–1997	59	±24 1950–1997	<i>65****</i>			10 %		Ice core	Oerter et al., 2000
G4	-70.9020	-0.4020	60	**		1983–2009	330	±21		-2 %		Ice core	Schlosser et al., 2014
M2	-70.3160	-0.1090	73	**		1981–2009	315	±22		-4 %		Ice core	Schlosser et al., 2014
G5	-70.5450	-0.0410	82	**		1983–2009	298	±21		-3 %		Ice core	Schlosser et al., 2014
K	-70.7500	0.0000	53	**		1954–1996	254	1980–1996	250	0 %		Ice core	Isaksson and Melvold, 2002
SPS	-90.0000	0.0000	2850	1816–1956	76.5	1965–1994	84.8	±3.3 1992–1997	84.5	±8.9	11 %	Ice core and poles	Mosley and Thompson, 1999
B32	-75.0023	0.0070	2882	1816–1997	63	1966–1997	80			27 %		Ice core	Oerter et al., 2000
EPICA DML	-75.0020	0.0680	2774	1915–2008	73	1964–2008	73.1	±1.7		0 %		Firn core and radar	Fujita et al., 2011
FB9808	-74.7507	0.9998	2860	1801–1997	68	±22 1950–1997	<i>74.5****</i>			10 %		Ice core	Oerter et al., 2000
FB9809	-74.4992	1.9608	2843	1801–1997	89	±29 1950–1997	<i>97.5****</i>			10 %		Ice core	Oerter et al., 2000
EPICA (Amundsenisen)	-75.0000	2.0000	2900	1865–1965	78	1966–1991	76			-3 %		Ice core	Isaksson et al., 1996
G8	-70.4100	2.0100	58	**		1991–2009	282	±26		-3 %		Ice core	Schlosser et al., 2014
FB9814	-75.0837	2.5017	2970	1801–1997	64	±21 1950–1997	<i>71****</i>			11 %		Ice core	Oerter et al., 2000
C	-72.2583	2.8911	2400	1955–1996	119	1965–1996	123			3 %		Ice core	Isaksson et al., 1999
D	-72.5083	3.0000	2610	1955–1996	112	1965–1996	116			4 %		Ice core	Isaksson et al., 1999
DML08	-75.7528	3.2828	2971	1919–96	60	*	<i>60</i>			0 %		Ice core	Oerter et al., 1999
E	-72.6750	3.6628	2751	1955–1996	55	1965–1996	59			7 %		Ice core	Isaksson et al., 1999

Site name	Latitude	Longitude	Elevation (m a.s.l.)	Last ~200 years	Accumulation (10 <sup>-3</sup> m w.e.) (kg m <sup>-2</sup> a <sup>-1</sup> )	Last ~50 years	Accumulation (10 <sup>-3</sup> m w.e.) (kg m <sup>-2</sup> a <sup>-1</sup> )	Last ~20 years	Accumulation (10 <sup>-3</sup> m w.e.) (kg m <sup>-2</sup> a <sup>-1</sup> )	% change (50a - ref)	% change (20a - ref) except**	Method	Study
DML02	-74.9683	3.9185	3027	1919–95	59 ±14 *		59			0 %		Ice core	Oerter et al., 1999
FB9810	-74.6672	4.0017	2980	1801–1997	86 ±29	1950–1997	94.5***			10 %		Ice core	Oerter et al., 2000
F	-72.8583	4.3514	2840	1955–1996	23	1965–1996	24			4 %		Ice core	Isaksson et al., 1999
S100	-70.2333	4.8000	48	1816–2000	292	1956–2000	284	1991–2000	260 ±80	-3 %	-11 %	Ice core	Kaczmarek et al., 2004
S20	-70.2417	4.8111	63	1955–1996	271	1965–1996	265			-2 %		Ice core	Isaksson et al., 1999
FB0601	-75.2470	4.8440	3090	1915–2008	52	1964–2008	51.6 ±1.2			-1 %		Firm core and radar	Fujita et al., 2011
FB9813	-75.1673	5.0033	3100	1816–1997	48	1950–1997	53***			10 %		Ice core	Oerter et al., 2000
G	-73.0417	5.0442	2929	1955–1996	28	1965–1996	30			7 %		Ice core	Isaksson et al., 1999
FB9804	-75.2503	6.0000	2630	1801–1997	50 ±16	1950–1997	55***			10 %		Ice core	Oerter et al., 2000
H	-73.3917	6.4606	3074	1955–1996	44	1965–1996	46			5 %		Ice core	Isaksson et al., 1999
B33	-75.1670	6.4985	3160	1816–1997	45.9	1966–1989	55			20 %		Ice core	Oerter et al., 2000, Sommer et al., 2000
FB9811	-75.0840	6.5000	3160	1801–1997	58 ±16	1950–1997	64***			10 %		Ice core	Oerter et al., 2000
DML09	-75.9333	7.2130	3156	1897–1996	45 ±12 *		45			0 %		Ice core	Oerter et al., 1999
DML10	-75.2167	7.2130	3364	1900–96	47 ±11 *		47			0 %		Ice core	Oerter et al., 1999
DML04	-74.3990	7.2175	3179	1905–1996	53 ±15 *		53			0 %		Ice core	Oerter et al., 1999
I	-73.8008	7.9406	3174	1955–1996	52	1965–1996	53			2 %		Ice core	Isaksson et al., 1999
NUS07-1	74.7200	7.9800	3174	1815–2007/8	52 ±2	1963–2007/8	55.9 ±3.9			8 %		Ice core	Anschutz et al., 2009
Site I	-73.7167	7.9833	3174	1815–2007	52 ±1.3	1963–2007	56 ±4.7	1991–2007	52	8 %	0 %	Ice core	Anschutz et al., 2009
DML06	-75.0007	8.0053	3246	1899–1996	50 ±14 *		50			0 %		Ice core	Oerter et al., 1999
NUS08-6	-81.7000	8.5700	2447	1815–2007/8	39.2 ±1.5	1963–2007/8	49.2 ±3.4			26 %		Ice core	Anschutz et al., 2011
J	-74.0417	9.4917	3268	1955–1996	44	1965–1996	45 ±4			2 %		Ice core	Isaksson et al., 1999
FB0603	-75.1170	9.7240	3300	1915–2008	41	1964–2008	38 ±0.9			-7 %		Firm core and radar	Fujita et al., 2011
K	-74.3583	11.1036	3341	1955–1996	45	1965–1996	41			-9 %		Ice core	Isaksson et al., 1999
L	-74.6417	12.7908	3406	1955–1996	45	1965–1996	41			-9 %		Ice core	Isaksson et al., 1999
A28	-74.8617	14.7420	3466	1915–2008	44	1964–2008	44.5 ±1			1 %		Firm core and radar	Fujita et al., 2011
MC	-75.0112	14.8865	3470.4	1816–1884	40	1955–2000	39	1992–2000	46	-3 %	15 %	Ice core	Karlof et al., 2005
MD	-74.9706	14.9567	3470.8	1816–1884	42	1955–2000	40	1992–2000	53	-5 %	26 %	Ice core	Karlof et al., 2005
M	-75.0000	14.9964	3470	1816–1884	41 ±0.7	1955–2000	41 ±0.5	1992–2000	50 ±1.1	0 %	22 %	Ice core	Karlof et al., 2005
M150	-74.9900	15.0000	3470	1816–1997	43	1965–1997	48.5			13 %		Ice core	Hofstede et al., 2004
M	-74.9917	15.0017	3453	1955–1965	51	1965–1996	45			-12 %		Ice core	Isaksson et al., 1999
MB	-75.0294	15.0435	3470.5	1816–1884	39	1955–2000	42	1992–2000	46	8 %	18 %	Ice core	Karlof et al., 2005
MA	-74.9887	15.1134	3470.4	1816–1884	42	1955–2000	42	1992–2000	48 ±1.3	0 %	14 %	Ice core	Karlof et al., 2005
NUS08-5	-82.6300	17.8700	2544	1815–2007/8	35 ±0.8	1963–2007/8	37.6 ±2.3			7 %		Ice core	Anschutz et al., 2011
NUS08-4	-82.8167	18.9000	2552	1815–2007/8	36.7 ±0.9	1963–2007/8	36.1 ±2.1			-2 %		Ice core	Anschutz et al., 2011
NUS08-3	-84.1300	22.0000	2625	1815–2007/8	40.1 ±1	1963–2007/8	45.3 ±3.1			13 %		Ice core	Anschutz et al., 2011
A35	-76.0660	22.4590	3586	1915–2008	35	1964–2008	39.2 ±0.9			12 %		Firm core and radar	Fujita et al., 2011
NUS07-2	-76.0700	22.4700	3582	1815–2007/8	33 ±0.7	1963–2007/8	28 ±2			-15 %		Ice core	Anschutz et al., 2011
MP	-75.8880	25.8340	3661	1286–2008	33.1 ±1.0	1964–2008	38.7 ±0.9	1993–2008	41.9 ±2.8	17 %	27 %	Firm core and radar	Fujita et al., 2011
NUS07-3	-77.0000	26.0500	3589	1815–2007/8	22 ±0.5	1963–2007/8	23.7 ±1.7			8 %		Ice core	Anschutz et al., 2009
IC12	-70.2458	26.3349	450	1816–2012	480 ±10	1955–2012	630 ±20	1992–2012	680 ±70	31 %	42 %	Ice core	This paper
DK190	-76.7940	31.9000	3741	1286–2008	28.7 ±0.9			1993–2008	34.1 ±2.3		19 %	Firm core and radar	Fujita et al., 2011
NUS07-4	-78.2167	32.8500	3595	1815–2007/8	19 ±0.5	1963–2007/8	17.5 ±1.2			-8 %		Ice core	Anschutz et al., 2009
NUS07-5	-78.6500	35.6300	3619	1815–2007/8	24 ±0.5	1963–2007/8	20.1 ±1.4			-16 %		Ice core	Anschutz et al., 2011
DF	-77.3170	39.7030	3810	1816–2001	26.3	1964–2008	28.8 ±0.7	1995–2006	27.3 ±0.4	10 %	4 %	Ice core	Igarashi et al., 2011
YM85	-71.5800	40.6300	2246	1816–2002	140	1965–2002	135			-4 %		Ice core	Takahashi et al., 2009
H72	-69.2047	41.0906	1214	1831–1998	311	1973–1998	307			-1 %		Ice core and poles	Nishio et al., 2002
NUS07-6	-80.7833	44.8500	3672	1815–2007/8	22	1902–2007/8	21			-5 %		Ice core	Anschutz et al., 2009
G15	-71.2000	45.9800	2544	1816–1964	86	1964–1984	116			35 %		Ice core	Moore et al., 1991
NUS07-8	-84.1833	53.5333	3452	1815–2007/8	32 ±1.2	1963–2007/8	30 ±2.1			-6 %		Ice core	Anschutz et al., 2009
NUS07-7	-82.0700	54.5500	3725	1815–2007/8	29.4 ±0.6	1963–2007/8	26.1 ±1.9			-11 %		Ice core	Anschutz et al., 2011
DT217	-75.7167	76.8333	2800	**		1998–2008	12 ±1.72	2005–2008	12		0 %	Stake arrays	Ding et al., 2011
DT364	-78.3333	77.0000	3380	**		1999–2008	62 ±0.14	2005–2008	72		16 %	Stake arrays	Ding et al., 2011

Site name	Latitude	Longitude	Elevation (m a.s.l.)	Last ~200 years Accumulation (10 <sup>-3</sup> m w.e.) (kg m <sup>-2</sup> a <sup>-1</sup> )	Last ~50 years Accumulation (10 <sup>-3</sup> m w.e.) (kg m <sup>-2</sup> a <sup>-1</sup> )	Last ~20 years Accumulation (10 <sup>-3</sup> m w.e.) (kg m <sup>-2</sup> a <sup>-1</sup> )	% change (50a - ref)	% change (20a - ref) except**	Method	Study		
DT401	-79.0200	77.0000	3760	1816–1999	19	1963–1999	24	1999–2005	25 ±16	26 %	32 % Ice core	Ren et al., 2010; Ding et al., 2011a
DT001	-70.8300	77.0700	2325	1810–1959	131	1959–1996	131			0 %	Ice core	Zhang et al., 2006
Dome A	-80.3667	77.3500	4093	**		2005–2008	19 ±0.25	2008–2009	21		11 % Stake arrays	Ding et al., 2011
DomeA	-80.3600	77.3600	4092	1815–1998	23	1963–1998	23			0 %	Ice core	Jiang et al., 2012
LGB65	-71.8500	77.9200	1850	1815–1996	131	1960–1996	131			0 %	Ice core	Xiao et al., 2004
DT008	-72.1667	77.9333	2390	**		1998–2008	118 ±0.30	2005–2008	80		-32 % Stake arrays	Ding et al., 2011
VOSTOK	-78.4500	106.8300	3488	1816–2010	20.6 ±0.3	1955–2010	21.5 ±0.5	1958–2010	20.8	4 %	1 % Snow pits and poles	Ekaykin et al., 2004
DSS	-66.7697	112.8069	1370	1816–2000	680	1970–2009	750			10 %	Ice core	Roberts et al., 2015
LAW DOME	-66.7700	112.9800	1370	1816–1966	687	1966–2005	742			8 %	Ice core	Morgan et al., 1991; van Ommen and Morgan, 2010
DomeC	-75.1200	123.3100	3233	1816–1998	25.3	1965–1998	28.3	1996–1998	39	12 %	54 % Ice core and poles	Frezzotti et al., 2005
D6 A	-75.4400	129.8100	3027	1816–1998	36 ±1.8	1966–1998	29 ±1.4	1998–2002	39	-19 %	8 % Ice core and poles	Frezzotti et al., 2005
D66	-68.9400	136.9400	2333	1966–1864	196	1965–2001	213 ±13	2001–2003	197	9 %	1 % Ice core and poles	Magand et al., 2004;Frezzotti et al., 2013
D2 A	-75.6200	140.6300	2479	1816–1998	20 ±1.0	1966–1998	31 ±1.6	1998–2002	30	55 %	50 % Ice core and poles	Frezzotti et al., 2005
GV1	-70.8700	141.3800	2244	1816–2001	114	1965–2001	117 ±7	2001–2003	96	3 %	-16 % Ice core and poles	Magand et al., 2004;Frezzotti et al., 2013
GV2	-71.7100	145.2600	2143	1816–2001	112	1965–2001	112 ±7	2001–2003	92	0 %	-18 % Ice core and poles	Magand et al., 2004;Frezzotti et al., 2013
MdPtA	-75.5300	145.8600	2454	1816–1998	36 ±1.8	1966–1998	45 ±2.7	1998–2010	47	25 %	31 % Ice core and poles	Frezzotti et al., 2005
GV3	-72.6300	150.1700	2137	1816–2001	81	1965–2001	84 ±5	2001–2003	73	4 %	-10 % Ice core and poles	Magand et al., 2004;Frezzotti et al., 2013
M2 A	-74.8000	151.2700	2278	1816–1998	17 ±0.8	1966–1998	15 ±7.5	1998–2002	8.5	-12 %	-50 % Ice core and poles	Frezzotti et al., 2005
GV4	-72.3900	154.4800	2126	1816–2001	119	1965–2001	100 ±6	2001–2003	96	-16 %	-19 % Ice core and poles	Magand et al., 2004;Frezzotti et al., 2013
31DPT A	-74.0300	155.9600	2069	1816–1998	98 ±4.9	1966–1998	112 ±5.6	1998–2002	98	14 %	0 % Ice core and poles	Frezzotti et al., 2005
GPS2A	-74.6400	157.5020	1804	1816–1998	60 ±3.0	1966–1998	54 ±2.7	1993–2000	55	-10 %	-8 % Ice core and poles	Frezzotti et al., 2005
GV5	-71.8900	158.5400	2184	1816–2001	129	1965–2001	129 ±7	2001–2004	135	0 %	5 % Ice core and poles	Magand et al., 2004;Frezzotti et al., 2007
GV7	-70.6800	158.8600	1947	1854–2001	237	1965–2001	241 ±13	2001–2004	252	2 %	6 % Ice core and poles	Magand et al., 2004;Frezzotti et al., 2007
Talos Dome	-72.7700	159.0800	2316	1816–2001	83.6	1966–1996	86.6	2001–2010	68	4 %	-19 % Ice core and poles	Magand et al., 2004;Frezzotti et al., 2007; 2013
Hercules Neve	-73.1000	165.4000	2960	1816–1966	118	1966–1992	129			9 %	Ice core	Stenni et al., 1999

## Supplementary materials

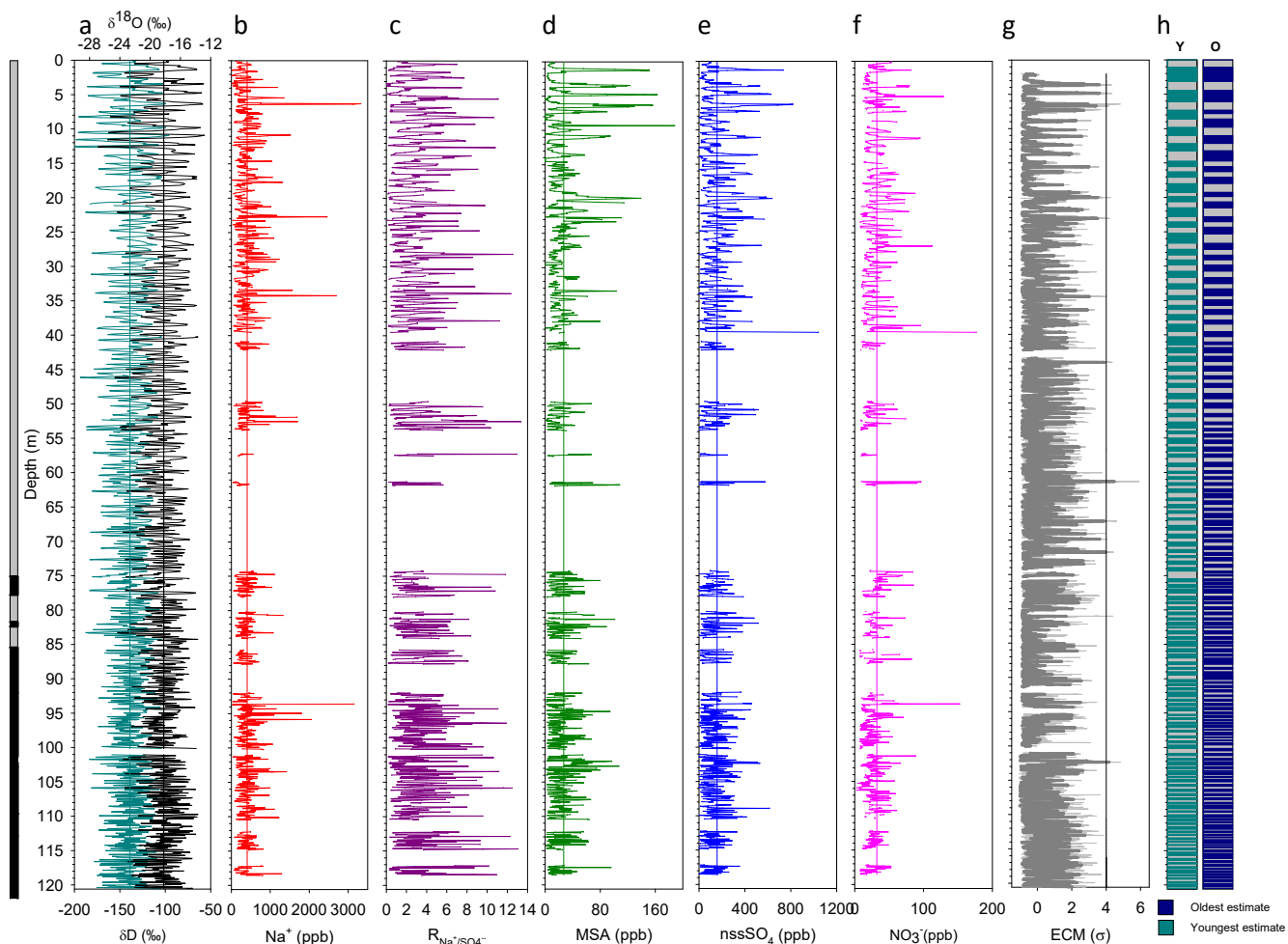


Fig. S1. Full vertical profile of water stable isotopes with a grey and black band on the left indicating sections of 10 cm and 5 cm resolution, respectively (a); major ion (b–f), normalized ECM conductivity expressed as multiple of standard deviation ( $\sigma$ ) (light grey: 1 mm resolution, dark grey: 0.05 m running mean). The  $4\sigma$  threshold is shown as a dotted vertical line, and identified volcanic peaks as dashed grey horizontal lines (g); annual layer boundaries in the youngest (Green) and the oldest (Blue) estimates. Each colour transition indicates a boundary (h).



Fig. S2. Full vertical profile, as in Fig. S1 but split in 17 sections for more visibility.

